Computers and Chemical Engineering 157 (2022) 107604

Contents lists available at ScienceDirect

Computers and Chemical Engineering

journal homepage: www.elsevier.com/locate/compchemeng

Framework for produced water discharge management with flow-weighted mean concentration based economic model predictive control

Otávio Fonseca Ivo*, Lars Struen Imsland

Department of Engineering Cybernetics, Norwegian University of Science and Technology, O.S. Bragstads plass 2, 7034 Trondheim, Norway

ARTICLE INFO

Article history:
Received 1 June 2021
Revised 8 October 2021
Accepted 16 November 2021
Available online 22 November 2021

Keywords:
Daily production optimization
Produced water re-injection
Economic model predictive control
Flow-weighted mean concentration

ABSTRACT

Offshore discharges of produced water (PW) is heavily regulated by government authorities through flow-weighted mean concentration (FWMC). To cope with regulations, treatment facilities are commissioned to reduce the oil content in water. However, disturbances may affect their performance, leading to regulation infringement. Produced water re-injection (PWRI) facilities can affect the FWMC by reducing oil discharge, and increasing re-injection. This strategy can aid the offshore facility in achieving the regulation requirements. Nevertheless, if improperly done, energy consumption can significantly increase, and regulations might still be violated. Therefore, we developed a framework for an Economical Model Predictive Control (EMPC) based on FWMC. It comprises an EMPC to which FWMCs are added as constraints; and a logic algorithm to maintain the necessary conditions for feasibility of the environmental constraint. Closed-loop results show that this strategy complies with environmental regulation, and adapts discharges of PW and pumping energy consumption based on facilities' historical data.

1. Introduction

Produced water (PW) is the highest by-product in terms of volume on the oil and gas industry. Generally, the amount of water in a new field is 2–4 times higher than the volume of oil and gas (Beyer et al., 2019). Nevertheless, as the field ages, the amount of PW increases as oil and gas are extracted, and PW is injected in the formation to maintain reservoir pressure for enhanced oil recovery (EOR). This phenomenon can be seen in the Norwegian continental shelf (NCS), as the growing number of older fields impacts the increased share of PW on the total output of oil and water (NOROG, 2019).

To limit the environmental impact of PW in oceans, standards and guidelines are imposed. According to regulations (Commision, 2001), no individual offshore installation should exceed a performance standard of 30 mg/L for the monthly average concentration of dispersed oil in PW. The monthly average or flow-weighted mean concentration (FWMC) of dispersed oil in PW should be calculated based on the results of at least 16 samples per month, which should be taken at equal time intervals. Moreover, the sampling location should be immediately after the last equipment in the treatment facility, and continuous monitoring may be used.

Norwegian regulators have announced the intention of lowering the performance standard from 30 mg/L to 10–15 mg/L for new field developments (Steinar et al., 2016), as it is known that oil in PW has the potential to create toxic effects and disturb the aquatic ecosystem near the discharging point. Moreover, oil exploration at the Barents Sea has been expanded recently (Kulovic, 2020). Current studies aim to elucidate if stricter regulations are needed for offshore activity in the Barents Sea/Arctic (Beyer et al., 2019). Nevertheless, it is still unclear if the biological species and ecosystems of these regions are more sensitive to toxic substances present in discharged PW than the ones in temperate waters (Beyer et al., 2020). In the following years, this topic will continue to receive attention from eco-toxicologists and regulators. For now, zero-adverse discharge police is the rule, and environmental risk assessment (ERA) must be performed (Smit et al., 2020). For current regulations and discharge standards in other regions of the world, one can consult Zheng et al. (2016).

To increase the environmental safety level of PW, management routines on oil and gas fields have to consider a four-step guideline (Miljdirektoratet, 2015):

* Corresponding author.
E-mail addresses: fonseca.i.otavio@ntnu.no (O.F. Ivo), lars.imsland@ntnu.no (L.S. Imsland).

https://doi.org/10.1016/j.compchemeng.2021.107604

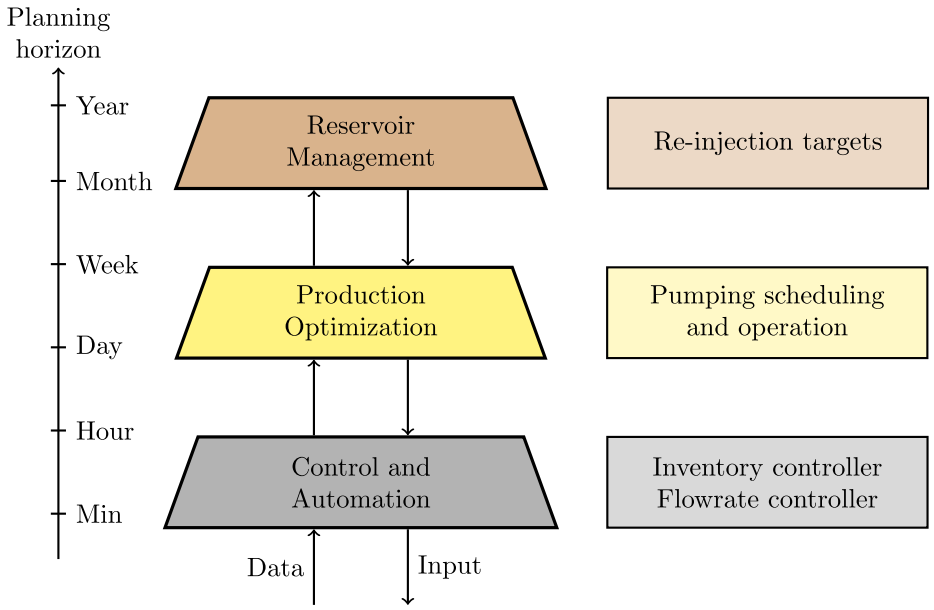

Fig. 1. Decision-making framework from the perspective of waterflooding operation.

- Avoid — Reduction of PW coming from well-streams through mechanical or chemical water shut-off (Taha and Amani, 2019).
- Prevent — Prevention of PW environmental harm by replacing production chemicals, choosing better design, and optimizing operation.
- Reduce — Reduction of discharges towards the ocean by injecting or re-injection of PW.
- Treat — Treating PW by removing oil and other environmentally hazardously components before discharging (Nasiri et al., 2017).

Coping with environmental requirements is a challenging task, especially at offshore processing plants as lack of space limits the range of treatment technologies available. Thus, it is not surprising that there is a preference for compact treatment methods (Judd et al., 2014). Operational improvements of such methods might be achieved by developing better control and optimization techniques as seen in Das and Jäschke, 2018, 2019, and Vallabhan et al. (2020). Nevertheless, several unavoidable factors are responsible for impacting the operational performance of treatment facilities (Steinar et al., 2016). For instance, the production profile of a reservoir evolves with time. Moreover, oil is extracted from a set of wells which may belong to different production zones. The summation of these factors can change the physicochemical properties of PW, which affect the performance of the treatment facility. In addition, frequency and duration of maintenance over separation equipment may lead to an unstable performance by the treatment facility (Steinar et al., 2016). When disturbances cause a decrease in the performance of the treatment facility, infringement of the monthly FWMC of dispersed oil in PW may occur.

The monthly FWMC of dispersed oil in PW depends on two factors: the concentration of dispersed oil in PW; and the flowrate of PW discharged in the ocean. While the treatment facility can manipulate the former, the produced water re-injection (PWRI) facility can manipulate the latter. Therefore, to better cope with environmental regulations, we advocate that the PWRI facility should actively manage the PW discharge policy. Nevertheless, one should be cautious when doing so. If PW management is improperly done, it can cause an increase in energy consumption and greenhouse gas (GHG) emissions without providing an improvement in the monthly FWMC of dispersed oil. In the worst case, the monthly FWMC of dispersed oil can even be violated. In this work, we have developed an Economic Model Predictive Control based on FWMC (FWMC-EMPC) to perform PW management. This controller is capable of coping with environmental regulations, while reducing considerably pumping energy consumption.

We structure the discussed topic as follows: In Section 2 we present a literature review on operation of PWRI and water distribution systems. In Section 3 we define some useful notations for a better understanding of the paper. In Section 4 we introduce the problem statement. The controller proposed in this work is presented in Section 5. In Section 6 we present the model of the PWRI facility network. In Section 7 we introduce the case studies used to benchmark the proposed controller. In Section 8 we discuss the results of each case study. Finally, we conclude this paper in Section 9.

2. Literature review

Produced water re-injection/injection or waterflooding is an enhanced oil recovery (EOR) approach used widely in the oil and gas industry. In Foss et al. (2018), a layered decision-making framework is presented for an oil and gas asset. In this work, we interpret this framework from the waterflooding perspective as shown in Fig. 1.

Reservoir management is at the top level in the hierarchy. To assist these decisions, reservoir engineers have at their disposition high fidelity reservoir models. This layer is mostly concerned with long term decisions that range from one to five years. As an output, daily re-injection targets are given to the production optimization layer. Several works in the literature have explored the optimization of reservoir management by considering the waterflooding system. The objective is generally to determine optimum re-injection and production settings to maximize the profitability of the venture using some performance indices such as net present value or total oil recovery. Some examples of research in this topic can be found in Grema and Cao (2013, 2016), Suwartadi et al. (2015), Hourfar et al. (2017), and Farajzadeh et al. (2019).

The production optimization layer has a planning horizon ranging from hours to weeks. Its main objective is to follow the daily re-injection targets while minimizing operational costs. In the pro-

duction optimization layer, it is important to account for the PW re-injection network. Many works developed for production optimization have considered the waterflooding daily optimization problem as a mixed-integer nonlinear programming (MINLP). In Zhang et al. (2017), a MINLP and a mixed-integer linear programming (MILP) were developed. The problem has been formulated to minimize the total operating energy consumption of the waterflooding facility, while considering the waterflooding station, wells and technical constraints. In addition, a comparison between derivative free and derivative based optimization methods was performed. In Zhou et al. (2019), a constraint that relates the water re-injection with the oil production was added to a MILP formulation.

On the lowest level, one can find the control and automation layer. Its main objective is to implement the production optimization strategy, which is achieved by control loops that use valves and variable-speed pumps to control flow rate and PW inventory. In Viholainen et al. (2013), a control strategy to improve energy efficiency of variable-speed pumps in parallel was presented. This strategy was developed based on real-time pump operation point estimation and selection of preferable operating area.

In the oil and gas industry, regulators are mainly concerned with a FWMC of dispersed oil in PW that ranges from days to one month (Zheng et al., 2016). Therefore, we propose that PW management should naturally be done by the production optimization layer due to its compatible time-scale. To the extent of this author knowledge, there is currently no formulation that has aimed to optimize a PWRI facility while accounting for the FWMC of dispersed oil in PW. Despite that, we acknowledge that water quality management is a topic of interest in the water distribution systems literature.

A review on water distribution operation can be found in Mala-Jetmarova et al. (2017). Some studies have focused on minimizing pumping operation time/costs while constraining the set of feasible solutions by adding water quality related constraints. Others have conducted multi-objective studies where in addition to operating costs, different variables associated with water quality were introduced in the objective function. As revealed by some of these studies, such as Arai et al. (2013) and Kurek and Ostfeld (2014), a trade-off involving water quality and operating costs do exist. For instance, in Arai et al. (2013), a fuzzy linear programming (LP) algorithm was developed to minimize multiple objectives associated with water supply, treatment, and distribution. Moreover, total organic carbon (TOC) was selected as a water quality indicator. The work of Kurek and Ostfeld (2014) considered two objectives in their formulation: reduce operating costs; and improve water quality. A penalty function based on the disinfectant concentration was used as the second objective. In Stentoft et al. (2020), where an EMPC problem was formulated, a threshold on the concentration of discharged nitrogen is imposed by adding constraints to the EMPC. Although a FWMC is mentioned in their work, it was never used in the EMPC formulation. In fact, what is included in the objective function is a daily taxation term based on the average mass of discharged nitrogen. In this work, we present an optimal control strategy that is capable of operating within the monthly discharge restrictions imposed by environmental regulators, achieving the required re-injection objectives, and minimize pumping energy consumption. We highlight that reduction of pumping energy leads to a decrease in GHG emission as the latter is proportional to the former. Values for GHG emissions can be obtained through the usage of emission factors; however, these factors were not considered in the present work since they are not part of its scope. For that, we refer to Stokes et al. (2015) as they have analyzed different emission factors to estimate GHG emissions of pumps in a water distribution system. Another important contribution of this work is on the development of the FWMC-EMPC. We present Theorem 1 which shows sufficient conditions for feasibility of FWMCs. This theorem is used in the construction of an EMPC with additional FWMC constraints, and in the construction of a logic algorithm for the development of the FWMC-EMPC framework. This formulation was inspired by Müller et al., 2014, which explored transient average in an EMPC framework.

3. Notation

We refer to the set of non-negative real numbers as $\mathbb{R}_{\geq 0}$, and the set of natural numbers as $\mathbb{N}$. The time domain is defined as $t \in \mathbb{R}_{\geq 0}$. Furthermore, we define fixed-times which are pre-established time constants and are represented as $t_m \in \mathbb{R}_{\geq 0}$, $\forall m \in \mathbb{N}$, with $t_m < t_{m+1}$. System variables use the notation $\cdot(t)$, while predictive variables use $\cdot(k|t_c)$, which denotes the k-step ahead prediction at the current time $t_c \in \mathbb{R}_{\geq 0}$. We use the accent $\tilde{(\cdot)}$ to indicate a FWMC variable, and the accent $\bar{(\cdot)}$ to indicate constants. An optimal solution is indicated by the superscript $(\cdot)^*$.

4. Problem statement

The system to be controlled is a semi-continuous operation. Its continuous part can be described by the set of index-1 differential algebraic equations (DAEs) described below,

$$\dot{x}(t) = f(x(t), z(t), u(t), w(t)), \tag{1a}$$

$$0 = g(x(t), z(t), u(t), w(t)), \tag{1b}$$

with nonlinear maps given by $f : \mathbb{R}^{n_x} \times \mathbb{R}^{n_z} \times \mathbb{R}^{n_u} \times \mathbb{R}^{n_w} \to \mathbb{R}^{n_x}$, and $g : \mathbb{R}^{n_x} \times \mathbb{R}^{n_z} \times \mathbb{R}^{n_u} \times \mathbb{R}^{n_w} \to 0$. Moreover, $x \in \mathbb{R}^{n_x}$ are dynamic states, $z \in \mathbb{R}^{n_z}$ are algebraic states, $u \in \mathbb{R}^{n_u}$ are control inputs, and $w \in \mathbb{R}^{n_w}$ are disturbances. The system is augmented with measurement outputs as follows,

$$c(t) = h_c(x(t), z(t), w(t)), \tag{1c}$$

$$q(t) = h_q(x(t), z(t), u(t), w(t)), \tag{1d}$$

where the output maps are given as $h_c : \mathbb{R}^{n_x} \times \mathbb{R}^{n_z} \times \mathbb{R}^{n_w} \to \mathbb{R}_{\geq 0}$, and $h_q : \mathbb{R}^{n_x} \times \mathbb{R}^{n_z} \times \mathbb{R}^{n_u} \times \mathbb{R}^{n_w} \to \mathbb{R}_{\geq 0}$, with $c \in \mathbb{R}_{\geq 0}$, and $q \in \mathbb{R}_{\geq 0}$ as concentration and flowrate outputs, respectively. Measurements of the system are assumed to be performed regularly. We define the expanding-time FWMC as a time-based weighted average evaluated from a fixed initial time t_m, to a variable final time t. The expanding-time FWMC is shown below,

$$\tilde{c}(t_m, t) = \frac{\mathbf{M}(t_m, t)}{\mathbf{V}(t_m, t)}, \tag{2a}$$

with,

$$\mathbf{M}(t_m, t) = \int_{t_m}^{t} c(\tau) q(\tau) d\tau, \tag{2b}$$

$$\mathbf{V}(t_m, t) = \int_{t_m}^{t} q(\tau)\ d\tau, \tag{2c}$$

where $\mathbf{M} : \mathbb{R}_{\geq 0} \to \mathbb{R}_{\geq 0}$ and $\mathbf{V} : \mathbb{R}_{\geq 0} \to \mathbb{R}_{\geq 0}$ are named as the total load map and the total volume map, respectively. Based on the expanding-time FWMC, we define the fixed-time FWMC, $\tilde{c}(t_m, t_{m+1}) \in \mathbb{R}_{\geq 0}$, which has a fixed initial and final time of integration. We use the previous definitions given for the expanding-time FWMC, and the fixed-time FWMC to create what we refer to as the piecewise expanding-time FWMC:

$$\tilde{c}(t) = \left\{ \tilde{c}(t_m, t), \quad \text{for } t_m < t \leq t_{m+1} \right\}, \quad \forall m \in \mathbb{N}, \tag{3}$$

where $\tilde{c}(t) \in \mathbb{R}_{\geq 0}$ is the piecewise expanding-time FWMC. Each fixed-time FWMC segment has a time interval $\Delta T_m = t_{m+1} - t_m$,

which is a few orders of magnitude longer than the settling time of system (1). The goal is to have the fixed-time FWMCs constrained in a particular region:

$$\tilde{c}(t_m, t_{m+1}) \in \mathbb{C}_f, \quad \forall m \in \mathbb{N}. \tag{4}$$

5. Flow-weighted mean concentration based EMPC

Economic model predictive control (Rawlings and Amrit, 2009), or dynamic-real time optimization (DRTO) (Kadam and Marquardt, 2007), is a predictive feedback control strategy where one aims to directly optimize an economic objective function over a certain prediction horizon by using the available degrees of freedom of a system (Rawlings and Amrit, 2009). In an EMPC, an optimal control problem is solved periodically with initial conditions given by the current state of the system. Such strategy is reminiscent of model predictive control (MPC), which has been widely adopted by the industry for set-point or trajectory tracking (Qin and Badgwell, 2003; Hrovat et al., 2012; Ferreau et al., 2016). Their main differences are their objective functions, theoretical proofs and area of application. Such differences are well covered in the literature (Faulwasser et al., 2018). Overall, EMPC can be considered flexible, robust, and its usage can lead to good economic performance. Moreover, it can potentially take economic advantage of disturbances in certain cases. Furthermore, one of its main strengths is that constraints over the inputs and states can be considered explicitly in its formulation (Rawlings et al., 2012). More information about EMPC can be found in Ellis et al. (2014). The FWMC-EMPC proposed in this work aims to guarantee feasibility of closed-loop fixed-time FWMCs. This formulation consists of a selector and two optimal control problems (OCP). One of which have extra constraints for guaranteeing feasibility of the closed-loop fixed-time FWMCs.

5.1. On the flow-weighted mean concentration properties

Before introducing the FWMC-EMPC, we present some properties of the expanding-time FWMC. Our aim is to show the mechanisms available for controlling the expanding-time FWMC through means of $q(t)$, which are later on used at the construction of an optimal control problem that can lead to the feasibility of the fixed-time FWMCs, $\tilde{c}(t_m, t_{m+1}) \in \tilde{\mathbb{C}}_f$, $\forall m \in \mathbb{N}$.

Proposition 1. *Suppose that $c(t) = \bar{c} \in \tilde{\mathbb{C}} \subseteq \mathbb{R}$. Then, for any $q(t) \in \mathbb{R}$ such that $\int_{t_m}^{t} q(t)\,dt \neq 0$, we have that $\tilde{c}(t_m, t) = \bar{c} \in \tilde{\mathbb{C}}$.*

Proof. The result follows directly by considering (2a) with $c(t) = \bar{c}$. Based on that, we have,

$$\tilde{c}(t_m, t) = \frac{\int_{t_m}^{t} c(t)q(t)\,dt}{\int_{t_m}^{t} q(t)\,dt} = \frac{\bar{c}\int_{t_m}^{t} q(t)\,dt}{\int_{t_m}^{t} q(t)\,dt} = \bar{c} \in \tilde{\mathbb{C}} \tag{5}$$

□

Remark 1. Based on Proposition 1, it is also possible to conclude that: if $c(t) = \bar{c} \notin \tilde{\mathbb{C}} \subseteq \mathbb{R}$, then $\tilde{c}(t_m, t) \notin \tilde{\mathbb{C}}$ for any $q(t) \in \mathbb{R}$ with $\int_{t_m}^{t} q(t)\,dt \neq 0$.

The previous proposition shows a case where the expanding-time FWMC is insensitive to changes in $q(t)$ as $\int_{t_m}^{t} q(t)\,dt \neq 0$. In fact, when $c(t)$ is a constant, the only control agency that one has over the expanding-time FWMC is whether $\int_{t_m}^{t} q(t)\,dt = 0 \vee \int_{t_m}^{t} q(t)\,dt \neq 0$. If $\int_{t_m}^{t} q(t)\,dt \neq 0$, feasibility of the expanding-time FWMC depends on whether $c(t) \in \tilde{\mathbb{C}} \vee c(t) \notin \tilde{\mathbb{C}}$. If $\int_{t_m}^{t} q(t)\,dt = 0$, feasibility of the expanding-time FWMC cannot even be discussed as its physical meaning is lost, and its mathematical function is now undefined. So far, we have considered that $c(t)$ remains constant for the whole $t \in \mathbb{R}_{\geq 0}$. Nevertheless, this is often not the case. As time passes, the controlled system is generally affected by disturbances, which in some cases might be persistent.

Proposition 2. *Consider that $\tilde{c}(t_m, t_c) \in \tilde{\mathbb{C}}$ with a $t_c \in [t_m, \infty)$. In addition, assume that $q(t) \in \mathbb{R}$. Then, for any $c(t) \in \mathbb{R}$ with $t \in (t_c, \infty)$, it is always possible to obtain $\tilde{c}(t_m, t) \in \tilde{\mathbb{C}}$.*

The result follow directly by choosing $q(t) = 0$, $t \in (t_c, \infty)$. In this case, we have from (2a) that:

$$\tilde{c}(t_m, t) = \frac{\mathbf{M}(t_m, t_c) + \cancelto{0}{\mathbf{M}(t_c, t)}}{\mathbf{V}(t_m, t_c) + \cancelto{0}{\mathbf{V}(t_c, t)}} = \tilde{c}(t_m, t_c) \in \tilde{\mathbb{C}}. \tag{6}$$

Remark 2. From a process standpoint, one can say that Proposition 2 reflects a simple notion: if one stops discharging a particular pollutant, the expanding-time FWMC will remain constant as time passes.

The previous proposition, reveals that as long as $\tilde{c}(t_m, t_c)$ is within the feasible region, it is sufficient to keep $q(t) = 0$ to maintain feasibility of the expanding-time FWMC for $t > t_c$. However, keeping future flowrates at zero does not necessarily lead to an optimal operation. Due to that, we would like to explore the behavior of expanding-time FWMC under less restrictive conditions.

Proposition 3. *Suppose that there exists a $t_\alpha \in [t_m, \infty)$, where $c(t) = \bar{c}_\alpha \in \mathbb{R}$. In addition, consider that $\lim_{t\to\infty} \int_{t_m}^{t} q(t)\,dt = \infty$. Then, for any $q(t) \in \mathbb{R}$, we have that $\lim_{t\to\infty} \tilde{c}(t_m, t) = \bar{c}_\alpha$.*

Proof. We start by taking the limit of (2a) with $t \to \infty$,

$$\lim_{t\to\infty} \tilde{c}(t_m, t) = \lim_{t\to\infty} \frac{\int_{t_m}^{t} c(t)q(t)\,dt}{\int_{t_m}^{t} q(t)\,dt}. \tag{7a}$$

We then split the integral at a $t_\alpha \in [t_m, \infty)$, and consider that $c(t) = \bar{c}_\alpha \in \mathbb{R}$:

$$\lim_{t\to\infty} \tilde{c}(t_m, t) = \lim_{\substack{t\to\infty \\ t>t_\alpha}} \frac{\int_{t_m}^{t_\alpha} c(t)q(t)\,dt + \int_{t_\alpha}^{t} \bar{c}_\alpha q(t)\,dt}{\int_{t_m}^{t} q(t)\,dt}. \tag{7b}$$

$$= \lim_{\substack{t\to\infty \\ t>t_\alpha}} \frac{\int_{t_m}^{t_\alpha} c(t)q(t)\,dt + \bar{c}_\alpha \int_{t_\alpha}^{t} q(t)\,dt}{\int_{t_m}^{t} q(t)\,dt} \tag{7c}$$

Assuming that $\lim_{t\to\infty} \int_{t_m}^{t} q(t) = \infty$, and that the first term is finite, one can obtain:

$$\lim_{t\to\infty} \tilde{c}(t_m, t) = \lim_{\substack{t\to\infty \\ t>t_\alpha}} \frac{\bar{c}_\alpha \int_{t_\alpha}^{t} q(t)\,dt}{\int_{t_m}^{t} q(t)\,dt}$$

$$= \lim_{\substack{t\to\infty \\ t>t_\alpha}} \frac{\bar{c}_\alpha \left(\int_{t_m}^{t} q(t)\,dt - \int_{t_m}^{t_\alpha} q(t)\,dt\right)}{\int_{t_m}^{t} q(t)\,dt} = \bar{c}_\alpha \tag{7d}$$

From (7d), one can conclude that,

$$\lim_{t\to\infty} \tilde{c}(t_m, t) = \bar{c}_\alpha, \tag{7e}$$

which is the end of the proof. □

Remark 3. Proposition 3 can also be translated from a process standpoint: if continuous discharge of a pollutant occurs where its concentration converges to a constant value, then the expanding-time FWMC will converge to this value as well.

Considering that there exist $t_c \in [t_m, \infty)$; $t_\alpha \in [t_c, \infty)$, where $c(t) = \bar{c}_\alpha \in \mathbb{R}$; and that $q(t) \in \mathbb{R}_{\geq 0}$ one can draw the following cases based on Propositions 2 and 3:

i. $\tilde{c}(t_m, t_c) \in \tilde{\mathbb{C}} \wedge \bar{c}_\alpha \in \tilde{\mathbb{C}} \Rightarrow \tilde{c}(t_m, t)$ will remain in $\tilde{\mathbb{C}}$.
ii. $\tilde{c}(t_m, t_c) \notin \tilde{\mathbb{C}} \wedge \bar{c}_\alpha \in \tilde{\mathbb{C}} \Rightarrow \tilde{c}(t_m, t)$ can converge to $\tilde{\mathbb{C}}$.
iii. $\tilde{c}(t_m, t_c) \in \tilde{\mathbb{C}} \wedge \bar{c}_\alpha \notin \tilde{\mathbb{C}} \Rightarrow \tilde{c}(t_m, t)$ can remain in $\tilde{\mathbb{C}}$.

iv. $\tilde{c}(t_m, t_c) \notin \tilde{\mathbb{C}} \wedge \bar{c}_\alpha \notin \tilde{\mathbb{C}} \Rightarrow \tilde{c}(t_m, t)$ cannot converge to $\tilde{\mathbb{C}}$.

Based on the cases shown above, it is clear that control actions have limited authority over the expanding-time FWMC as converging $\tilde{c}(t_m, t)$ to $\tilde{\mathbb{C}}$ is dependent on whether $\tilde{c}(t_m, t_c) \in \tilde{\mathbb{C}}$ or $\bar{c}_\alpha \in \tilde{\mathbb{C}}$. Based on that, we propose the following Theorem:

Theorem 1. *(Necessary conditions of feasibility) Suppose that there exist a $\tilde{c}(t_m, t_c) \in \mathbb{R}$ with $t_m \in \mathbb{R}_{\geq 0}$ and $t_c \in (t_m, \infty)$. Moreover, that $\lim_{t\to\infty} c(t) = \bar{c} \in \mathbb{R}$. Then, to obtain $\tilde{c}(t_m, t_\alpha) \in \tilde{\mathbb{C}}$ for a $t_\alpha \in (t_c, \infty)$, it is necessary that at least one of the following two conditions holds:*

(i) $\tilde{c}(t_m, t_c) \in \tilde{\mathbb{C}}$.
(ii) $\lim_{t\to\infty} c(t) \in \tilde{\mathbb{C}}$.

We have seen that the fixed-time FWMC is a specific case of the expanding-time FWMC. Thus, we make some remarks about each criterion of Theorem 1, and its applicability when one wants to obtain $\tilde{c}(t_m, t_{m+1}) \in \tilde{\mathbb{C}}_f$. For these remarks, we consider that $\tilde{\mathbb{C}} = \tilde{\mathbb{C}}_f$.

Remark 4. Criterion (i) is concerned with the past behavior of the expanding-time FWMC. If only this condition holds, then the expanding-time FWMC departs from $\tilde{c}(t_m, t_c) \in \tilde{\mathbb{C}}$ and can eventually leave region $\tilde{C}$ at a time $t \in (t_c, \infty)$. However, as long as it is possible to select a set of control actions to keep $\tilde{c}(t_m, t) \in \tilde{\mathbb{C}}$ for $t \in (t_c, \infty)$, then $\tilde{c}(t_m, t_{m+1}) \in \tilde{\mathbb{C}}$. Imposition of $\tilde{c}(t_m, t) \in \tilde{\mathbb{C}}$ for $t \in (t_c, \infty)$ implicitly restrict the original set of allowable control actions to a particular subset, which could affect negatively the economic performance of the closed-loop system.

Remark 5. Criterion (ii) focus on the future behavior of the expanding-time FWMC. If only this condition holds, then $\tilde{c}(t_m, t_c) \notin \tilde{\mathbb{C}}$. From Proposition 3, we have that $\lim_{t\to\infty} \tilde{c}(t_m, t) \in \tilde{\mathbb{C}}$ given a set of assumptions. If economic improvements in the system can be found when $c(t_m, t) \notin \tilde{\mathbb{C}}$, then the economic performance of the closed-loop system can be positively affected by operating outside the region $\tilde{\mathbb{C}}$ for a while. However, the exact time t_α in which $\tilde{c}(t_m, t_\alpha) \in \tilde{\mathbb{C}}$ is unclear. Thus, one can have $\tilde{c}(t_m, t_{m+1}) \in \tilde{\mathbb{C}} \vee \tilde{c}(t_m, t_{m+1}) \notin \tilde{\mathbb{C}}$. The latter outcome is clearly undesirable as feasibility of $\tilde{c}(t_m, t_{m+1})$ is not achieved.

Compared with criterion (i), criterion (ii) enforces less constrains on the set of allowable control actions. Moreover, criterion (ii) enables one to operate for some time with $\tilde{c}(t_m, t) \notin \tilde{\mathbb{C}}$, which might be economically beneficial for the closed-loop system. However, exploiting criterion (ii) and these economic benefits is problematic to say the least. First, it is necessary to know the values of $c(t)$ for $t \in (t_c, t_{m+1}]$, which can be quite challenging due to plant-model mismatch, or disturbances. Second, future values of $c(t)$ should be within the region $\tilde{\mathbb{C}}$. Third, there should be enough time left for the expanding-time FWMC to go from $\tilde{c}(t_m, t_c) \notin \tilde{\mathbb{C}}$ to $\tilde{c}(t_m, t_{m+1}) \in \tilde{\mathbb{C}}$. Due to these issues, we focus on designing an OCP based on criterion (i) in the next section.

5.2. Optimal control problem formulation

The proposed OCP should be able to minimize a stage cost $\ell : \mathbb{R}^{n_x} \times \mathbb{R}^{n_z} \times \mathbb{R}^{n_u} \to \mathbb{R}$, which is assumed to be an economic cost. Moreover, it would be desired to maintain the states, control actions, and fixed-time FWMCs at particular bounded regions of the Euclidean space, such that:

$$\begin{aligned} &\mathbb{X} \in \mathbb{R}^{n_x},\ \mathbb{Z} \in \mathbb{R}^{n_z},\ \mathbb{U} \in \mathbb{R}^{n_u},\ \tilde{\mathbb{C}}_f \in \mathbb{R}, \\ &(x(t), z(t), u(t)) \in \mathbb{X} \times \mathbb{Z} \times \mathbb{U}, \\ &\tilde{c}(t_m, t_{m+1}) \in \tilde{\mathbb{C}}_f, \qquad \forall m \in \mathbb{N}. \end{aligned} \tag{8}$$

In the previous subsection, necessary conditions of feasibility were obtained for the expanding-time FWMC. Furthermore, we have discussed the implication of Theorem 1 with respect to a fixed-time FWMC. We have decided to formulate an OCP based on condition (i) of Theorem 1 to optimally control the system (1a)–(3). The main reason for making this choice is that condition (ii) is associated with future realizations of the system behavior which are generally unknown or partially known, thus considered unreliable. Based on the above, the OCP_F used in the FWMC-EMPC is:

$$\min_{u(t)} \quad \int_{t_c}^{t_p} \ell(x(\tau|t_c), z(\tau|t_c), u(\tau|t_c))\, d\tau, \tag{9a}$$

$$s.t. \quad \dot{x}(t|t_c) = f(x(t|t_c), z(t|t_c), u(t|t_c), w(t|t_c)), \tag{9b}$$

$$0 = g(x(t|t_c), z(t|t_c), u(t|t_c), w(t|t_c)), \tag{9c}$$

$$\dot{w}(t|t_c) = f_d(w(t|t_c)), \tag{9d}$$

$$(x(t|t_c), z(t|t_c), u(t|t_c)) \in \mathbb{X} \times \mathbb{Z} \times \mathbb{U}, \tag{9e}$$

$$x(0|t_c) = \bar{x}_c,\ w(0|t_c) = \bar{w}_c, \tag{9f}$$

$$c(t|t_c) = h_c(x(t|t_c), z(t|t_c), w(t|t_c)), \tag{9g}$$

$$q(t|t_c) = h_q(x(t|t_c), z(t|t_c), u(t|t_c), w(t|t_c)), \tag{9h}$$

$$\tilde{c}(t_m, t_c + k \cdot T|t_c) \in \widetilde{\mathbb{C}},\ k \in \mathbb{N}_{[1,N]} \tag{9i}$$

with,

$$\tilde{c}(t_m, t_c + k \cdot T|t_c) = \frac{\mathbf{M}(t_m, t_c) + \mathbf{M}(t_c, t_c + k \cdot T|t_c)}{\mathbf{V}(t_m, t_c) + \mathbf{V}(t_c, t_c + k \cdot T|t_c)}, \tag{9j}$$

and,

$$\mathbf{M}(t_c, t_c + k \cdot T|t_c) = \int_{t_c}^{t_c + k \cdot T} q(\tau|t_c) c(\tau|t_c)\, d\tau, \tag{9k}$$

$$\mathbf{V}(t_c, t_c + k \cdot T|t_c) = \int_{t_c}^{t_c + k \cdot T} q(\tau|t_c)\, d\tau, \tag{9l}$$

where $t_p := T \cdot N + t_c$ is the prediction time; N is the prediction horizon; and T is the FWMC look-ahead time. Moreover, (9a) is the objective function; (9b) is the dynamic model; (9c) is the algebraic model; (9d) is the disturbance model; (9e) is the states and control input bounds; (9f) is the initial values; (9g) is the concentration output model; (9h) is the flowrate output model; and (9i) are bounds associated with the expanding-time FWMC, which is described by (9j)-(9l).

The OCP_F shown in (9) is parametric in the initial states $(\bar{x}_c; \bar{w}_c)$, and past behavior of the FWMC $(\mathbf{M}(t_m, t_c); \mathbf{V}(t_m, t_c))$. Its main novelty is the inclusion of (9i), which accounts for N constraints. Each of these constraints limits the expanding-time FWMC to the region $\tilde{\mathbb{C}}$. However, to properly predict the system behavior, some additional models are necessary. For instance, (9i) requires a model for the output maps $h_c(\cdot)$, and $h_q(\cdot)$. Moreover, a disturbance model is considered, as the closed-loop performance is directly affected by disturbances. To obtain such models, one could use offset free EMPC (Morari and Maeder, 2012; Pannocchia, 2015). Nevertheless, in this work, we assume the following disturbance model,

$$\dot{w}(t|t_c) = 0. \tag{10}$$

The set of admissible control inputs based on OCP (9) is defined as follows, $\mathcal{U} := \{u(t|t_c) \mid (9b), \ldots, (9i)\}$. By considering a receding horizon approach (Mayne and Michalska, 1988), one obtains the following implicit control law, $u_N^*(x(t), w(t), \mathbf{M}(t_m, t), \mathbf{V}(t_m, t)) := \kappa_N(x(t), w(t), \mathbf{M}(t_m, t), \mathbf{V}(t_m, t))$. We refer to the application of such control law to the system of equations (1a)-(2a):

$$\dot{x}(t) = f(x(t), z(t), u_N^*(x(t), w(t), \mathbf{M}(t_m, t), \mathbf{V}(t_m, t)), w(t)), \tag{11a}$$

$$0 = g(x(t), z(t), u_N^*(x(t), w(t), \mathbf{M}(t_m, t), \mathbf{V}(t_m, t)), w(t)), \tag{11b}$$

with measurement output as,

$$c(t) = h_c(x(t), z(t), w(t)), \tag{11c}$$

$$q(t) = h_q(x(t), z(t), u_N^*(x(t), w(t), M(t_m, t), V(t_m, t)), w(t)), \tag{11d}$$

and piecewise expanding-time FWMC,

$$\tilde{c}(t) = \left\{ \tfrac{\mathbf{M}(t_m,t)}{\mathbf{V}(t_m,t)}, \quad \text{for } t_m < t \leq t_{m+1} \right\}, \quad \forall m \in \mathbb{N}, \tag{11e}$$

From the closed-loop system shown in (11a)–(11e) it is possible to see how historical information from the piecewise expanding-time FWMC is used by the OCP_F (9). We show below that as long as $c(t_m) \in \tilde{\mathbb{C}}$, then condition (i) of Theorem 1 hold for the closed-loop system. The shortest expanding-time FWMC is given below:

$$\lim_{\delta t \to 0} \tilde{c}(t_m, t_m + \delta t) = \lim_{\delta t \to 0} \frac{\int_{t_m}^{t_m+\delta t} q(\tau) c(\tau)\, d\tau}{\int_{t_m}^{t_m+\delta t} q(\tau)\, d\tau}, \tag{12a}$$

which is indeterminate. By manipulating (12a) and applying L'Hôpital's rule, the following is obtained:

$$\lim_{\delta t \to 0} \tilde{c}(t_m, t_m + \delta t) = \lim_{\delta t \to 0} \frac{q(t_m + \delta t) c(t_m + \delta t)}{q(t_m + \delta t)} = c(t_m). \tag{12b}$$

Considering that constraints (9i) embeds condition (i) of Theorem 1 to the OCP_F, and assuming that $c(t_m) \in \tilde{\mathbb{C}}$, then the piecewise expanding-time FWMC remains in the region $\tilde{\mathbb{C}}$ when the control law $u_N^*(x(t), w(t), \mathbf{M}(t_m, t), \mathbf{V}(t_m, t))$ is used.

5.3. Practicalities of the FWMC-EMPC

In the previous subsection, it was shown that the closed-loop piecewise expanding-time FWMC remains in the region $\tilde{\mathbb{C}}$ if $c(t_m) \in \tilde{\mathbb{C}}$. However, in practice, this condition will not always be true. In reality, disturbances affecting the system can be such that $c(t_m) \notin \tilde{\mathbb{C}}$. Under this condition, then criterion (i) of Theorem 1 ceases to hold and OCP_F (9) might not find a feasible solution due to constraints (9i). To solve the aforementioned issue, one can soften constraints (9i) by adding slack variables (Kerrigan and Maciejowski, 2000), which creates the OCP_S. Soft constraints have the purpose of penalizing violations over particular constraints. More specifically, they should be used in constraints that could but should not be violated. This enables one to still solve an OCP similar to OCP_F (9), in which minimal violation over (9i) is enforced. While $\tilde{c}(t_m, t)$ with $t \in (t_m, t_{m+1})$ can be violated in the closed-loop, violation of $\tilde{c}(t_m, t_{m+1})$ is highly undesirable. As shown in Theorem 1, when criterion (i) does not hold, then criterion (ii) must hold for one to be able to reach the region $\tilde{\mathbb{C}}$. As discussed earlier in this work, relying on criterion (ii) might not be the best option. To avoid loss of criterion (i) in the first place, we propose the usage of the following Algorithm:

On this algorithm, there are two *if* clauses. The first *if* checks if a new period $[t_m, t_{m+1})$ has begun. If it has, then *criteria* is set to be *True*. The second *if* has two clauses to check if criterion (i) of Theorem 1 holds. The first clause checks if $c(t_c) \in \tilde{\mathbb{C}}$ or OCP_F has been previously solved. If one of them is true, the OCP_F is solved and *criteria* is set as true. Thus, until the end of the month, the OCP_F becomes the only available strategy. If both clauses are false, then OCP_R is solved. As mentioned previously in this work, the physical meaning of the FWMC is lost when $q(t|t_c)$ is set to zero. Due to that, feasibility of the expanding-time FWMC cannot even be discussed. Therefore, OCP_R has the role of delaying the evaluation of the expanding-time FWMC until criterion (i) of Theorem 1 is met. The OCP_R consists of Eqs. (9a)–(9f), (9h) and the additional constraint $q(t|t_c) = 0$. It is important to highlight that the algorithm presented in this section assumes that once OCP_F has been solved, then criterion (i) of Theorem 1 holds in the closed-loop system. In practice, this assumption may not hold due to plant-model mismatch and/or unknown disturbances. For these cases, one may couple to OCP_F approaches that take these issues into account while still keeping the value of Algorithm 1 .

Algorithm 1: FWMC-EMPC.

Input: $t_m, t_{m+1}, t_c, x(t_c), w(t_c), \mathbf{M}(t_m, t_c), \mathbf{V}(t_m, t_c), criteria$
Output: $u(t|t_c)$
if $t_c = t_m$ **then**
  $criteria \leftarrow True$
end
if $c(t_c) \in \tilde{\mathbb{C}}$ **or** $criteria = False$ **then**
  $u(t|t_c) \leftarrow$ solve $\text{OCP}_F(x(t_c), w(t_c), \mathbf{M}(t_m, t_c), \mathbf{V}(t_m, t_c))$
  $criteria \leftarrow False$
else
  $u(t|t_c) \leftarrow$ solve $\text{OCP}_R(x(t_c), w(t_c), 0, 0)$
end

5.4. Numerical issues of the OCP

To solve an OCP, one should use numerical methods for trajectory optimization. In this work, we consider direct transcription by orthogonal collocation (Biegler, 2010). Through this method, a trajectory optimization problem is transcribed into a nonlinear program (NLP), which must be solved by using a NLP solver. NLP solvers are iterative in nature, and in essence use Newton's method. Furthermore, most NLP solvers are built with the assumption that certain constraint qualifications hold. For a detailed survey over different trajectory optimization methods, one can refer to Betts (1998). For optimization algorithms, we refer to Nocedal and Wright (2006). We present a compact form of a NLP resulting from direct transcription of OCP_F or OCP_S:

$$\min_{\boldsymbol{\theta}} \quad \Phi(\boldsymbol{\theta}, \mathbf{p}) \tag{13a}$$

$$s.t. \quad \mathbf{g}(\boldsymbol{\theta}, \mathbf{p}) = 0, \tag{13b}$$

$$\mathbf{h}(\boldsymbol{\theta}, \mathbf{p}) \leq 0, \tag{13c}$$

where (13a) is the objective function $\Phi : \mathbb{R}^{n_\theta} \times \mathbb{R}^{n_p} \to \mathbb{R}$; (13b) are equality constraints $\mathbf{g} : \mathbb{R}^{n_\theta} \times \mathbb{R}^{n_p} \to \mathbb{R}^{n_g}$; and (13c) is a vector of inequality constraints $\mathbf{h} : \mathbb{R}^{n_\theta} \times \mathbb{R}^{n_p} \to \mathbb{R}^{n_h}$, with $\boldsymbol{\theta} \in \mathbb{R}^{n_\theta}$ as decision variables and $\mathbf{p} \in \mathbb{R}^{n_p}$ as parameters. The constraint (9i) present in (9) imposes numerical challenges for a NLP solver. While some issues can be addressed by reformulating (13), others cannot. Below, we describe the issues associated with NLP_F and NLP_S. We stress that although NLP_S has the presence of soft-constraints and slack variables, it does not affect the following analysis. Consider that (13) has the following variables as elements of the vectors $\boldsymbol{\theta}$ and $\mathbf{p}$:

$$\theta_{c,k} = \tilde{c}(t_m, t_c + k \cdot T|t_c), \quad \forall k \in \mathbb{N}_{[1,N]}, \tag{14a}$$

$$\theta_{m,k} = \mathbf{M}(t_c, t_c + k \cdot T | t_c), \quad \forall k \in \mathbb{N}_{[1,N]}, \tag{14b}$$

$$\theta_{v,k} = \mathbf{V}(t_c, t_c + k \cdot T | t_c), \quad \forall k \in \mathbb{N}_{[1,N]}, \tag{14c}$$

$$p_m = \mathbf{M}(t_m, t_c), \tag{14d}$$

$$p_v = \mathbf{V}(t_m, t_c), \tag{14e}$$

where $\theta_{c,k}$, $\theta_{m,k}$, and $\theta_{v,k}$ are decision variables; and p_m and p_v are parameters. Moreover, that constraint (9j) is represented as,

$$\theta_{c,k} - \frac{p_m + \sum_{j=1}^{k} \theta_{m,j}}{p_v + \sum_{j=1}^{k} \theta_{v,j}} = 0, \quad \forall k \in \mathbb{N}_{[1,N]}, \tag{15}$$

and the following inequalities are part of (13),

$$\theta_{v,k} \geq 0, \ \theta_{m,k} \geq 0, \quad \forall k \in \mathbb{N}_{[1,N]}, \tag{16}$$

We have that constraints in (15) are undefined when their denominators are equal to zero. To avoid such issue, those constraints are reformulated as,

$$\theta_{c,k}\left(p_v + \sum_{j=1}^{k} \theta_{v,j}\right) - \left(p_m + \sum_{j=1}^{k} \theta_{m,j}\right) = 0, \quad \forall k \in \mathbb{N}_{[1,N]}, \tag{17}$$

which are now fully defined. Although this modification solves the ratio issue, we indicate that under some conditions, the gradient of equality constraints in NLP_F can lose its rank, causing Linear Independence Constraint Qualification (LICQ) to not be satisfied. This has major consequences over convergence of most NLP solvers as satisfaction of the LICQ is an important property that must hold while solving a NLP. In the next paragraph, we show how LICQ can cease to hold for this new formulation. The equality constraint (17) is the only one in which $\theta_{c,k}$ is present. Thus, $\nabla_{\theta_{c,k}} \mathbf{g}(\boldsymbol{\theta}, \mathbf{p})$ have only one non-zero element, which is given below,

$$\nabla_{\theta_{c,k}}(17) = p_v + \sum_{j=1}^{k} \theta_{v,j}, \quad \forall k \in \mathbb{N}_{[1,N]}. \tag{18}$$

Due to inequalities (16), the following conditions hold true,

$$p_v + \sum_{j=1}^{k} \theta_{v,j} \leq p_v + \sum_{j=1}^{k+1} \theta_{v,j}, \quad \forall k \in \mathbb{N}_{[1,N-1]}, \tag{19}$$

which reveals that $p_v + \theta_{v,1} = 0$ is sufficient for $\nabla \mathbf{g}(\boldsymbol{\theta}, \mathbf{p})$ to lose a rank. As shown in (16), $\theta_{v,k}$ is non-negative. Thus, it is necessary to have both p_v and $\theta_{v,1}$ different from zero for the LICQ to hold. One must be aware that all the elements in NLP (13) play a role on whether $\theta^*_{v,1} = 0$ is a local optimum of either NLP_F or NLP_S when $p_v = 0$. Thus, depending on the nature of the original problem, the underlined issue might not emerge.

6. Process description

The objective of a PWRI facility is to re-inject the required amount of PW in the formation to maintain reservoir pressure for EOR. To perform that, PW needs to be boosted by pumps to achieve the required re-injection flowrate. In this process, energy is consumed and GHGs are emitted. The required flowrate of PW to be re-injected in each individual well is usually set by reservoir engineers. If more PW is available, it is common to discharge it towards the ocean. Discharged PW contains a small concentration of dispersed oil, and monthly discharges based on FWMC are heavily regulated by governmental authorities. Based on this brief description, we state that it is desired to minimize energy consumption, comply with the environmental regulation, and re-inject the required PW at re-injection wells.

Table 1
Definition of nodal-arc sets.

Symbol	Description
$\mathcal{J}_T \in \mathcal{J}$	Set containing tanks.
$\mathcal{J}_D \in \mathcal{J}$	Set containing discharges.
$\mathcal{J}_W \in \mathcal{J}$	Set containing wells.
$\mathcal{J} = \mathcal{J}_T \cup \mathcal{J}_D \cup \mathcal{J}_W$	Set containing all the nodes in a network.
$\mathcal{L}_D \in \mathcal{L}$	Set containing discharging lines.
$\mathcal{L}_P \in \mathcal{L}$	Set containing pumping facilities.
$\mathcal{L} = \mathcal{L}_D \cup \mathcal{L}_P$	Set containing all the arcs in a network.

6.1. Notation and variables

In the water distribution and production optimization literature, it is common to represent a distribution system by means of a graph network. In this work, we assume a directional graph network $\mathcal{G} = (\mathcal{J}, \mathcal{L})$, where $\mathcal{J} := \{i \mid \forall i \in 1, \ldots, n_n\}$ is the set of nodes, and $\mathcal{L}$ the set of arcs. We refer to an individual node as $i \in \mathcal{J}$, and append a subscript $(\cdot)_i$ to its variables. In addition, we refer to an individual arc as $l \in \mathcal{L}$, and append a subscript $(\cdot)_l$ to its variables. As an arc is responsible for connecting a source node to a target node, it is also possible to identify an individual arc $l \in \mathcal{L}$ by replacing l with the tuple (i, j) or (j, i), where (i, j) represents from node i to j, and (j, i) from node j to i. Both sets $\mathcal{J}$ and $\mathcal{L}$ can be divided in disjoint subsets which represent the elements of a facility. In Table 1, we introduce the definition of each disjoint subset used in this work, with an explanation of which element of the facility is being considered.

We consider that the facility can be modeled as a DAE system with index-1, which is shown below in its implicit form:

$$\mathbf{0} = \mathbf{F}(\dot{\mathbf{x}}, \mathbf{x}, \mathbf{z}, \mathbf{u}, \mathbf{w}, \mathbf{p}), \tag{20}$$

in which the $\mathbf{F} : \mathbb{R}^{n_x} \times \mathbb{R}^{n_z} \times \mathbb{R}^{n_u} \times \mathbb{R}^{n_w} \times \mathbb{R}^{n_p} \to \mathbf{0}$ is a nonlinear map, where $\mathbf{x}$ is a vector of dynamic states; $\mathbf{z}$ is a vector of algebraic states; $\mathbf{u}$ is a vector of control inputs; $\mathbf{w}$ is a vector of disturbances; and $\mathbf{p}$ is a vector of parameters. We define these vectors as follows,

$$\mathbf{x} = \begin{bmatrix} \mathbf{x}_{\text{node}}^T & \mathbf{x}_{\text{arc}}^T \end{bmatrix}^T, \tag{21a}$$

$$\mathbf{z} = \begin{bmatrix} \mathbf{z}_{\text{node}}^T & \mathbf{z}_{\text{arc}}^T \end{bmatrix}^T, \tag{21b}$$

$$\mathbf{u} = \begin{bmatrix} \mathbf{u}_{\text{node}}^T & \mathbf{u}_{\text{arc}}^T \end{bmatrix}^T, \tag{21c}$$

$$\mathbf{w} = \begin{bmatrix} \mathbf{w}_{\text{node}}^T & \mathbf{w}_{\text{arc}}^T \end{bmatrix}^T, \tag{21d}$$

$$\mathbf{p} = \begin{bmatrix} \mathbf{p}_{\text{node}}^T & \mathbf{p}_{\text{arc}}^T \end{bmatrix}^T, \tag{21e}$$

where $\mathbf{x}_{\text{node}}$, $\mathbf{z}_{\text{node}}$, $\mathbf{u}_{\text{node}}$, $\mathbf{w}_{\text{node}}$, and $\mathbf{p}_{\text{node}}$ are respectively node vectors; and $\mathbf{x}_{\text{arc}}$, $\mathbf{z}_{\text{arc}}$, $\mathbf{u}_{\text{arc}}$, $\mathbf{w}_{\text{arc}}$, and $\mathbf{p}_{\text{arc}}$ are respectively arc vectors. Furthermore, both node and arc vectors are formed by a collection of individual node vectors $(\cdot)_i \in \mathcal{J}$, and individual arc vectors $(\cdot)_l \in \mathcal{L}$. Before presenting such vectors, we exhibit Table 2, in which we define the physical variable present in the network model.

The vector of an individual node $i \in \mathcal{J}$ is defined as follows. For tank nodes $\mathcal{J}_T$, there is:

$$\mathbf{x}_i = \begin{bmatrix} V_i \end{bmatrix}^T, \quad \forall i \in \mathcal{J}_T, \tag{22a}$$

Table 2
Definition of the physical variables present in the network model.

Symbol	Unit	Description	
γ_i	N/m^3	PW specific weight at node i,	$\forall i \in \mathcal{J}$
c_i	kg/m^3	Concentration of dispersed oil at node i,	$\forall i \in \mathcal{J}_W$
d_i	m^3/s	Demand at node i,	$\forall i \in \mathcal{J}$
d_i^o	kg/s	Oil demand at node i,	$\forall i \in \mathcal{J}_W$
h_i	m	Liquid level at node i,	$\forall i \in \mathcal{J}_T$
q_l	m^3/s	Volumetric flowrate at arc l,	$\forall l \in \mathcal{L}$
p_i	Pa	Pressure at node i,	$\forall i \in \mathcal{J}$
p_i^r	Pa	Reservoir pressure at node i,	$\forall i \in \mathcal{J}_W$
p_i^s	Pa	Pressure at the surface of node i,	$\forall i \in \mathcal{J}_T$
z_i	m	Elevation at node i,	$\forall i \in \mathcal{J}$
z_o	m	Reference elevation	
H_i	m	Hydraulic head at node i,	$\forall i \in \mathcal{J}$
J_i	m^3/sPa	Injectivity index at node i,	$\forall i \in \mathcal{J}_W$
V_i	m^3	Volume at node i,	$\forall i \in \mathcal{J}_T$
W_l	W	Hydraulic power demand at arc l,	$\forall l \in \mathcal{L}$

$$\mathbf{z}_i = \begin{bmatrix} p_i & H_i & h_i \end{bmatrix}^T, \quad \forall i \in \mathcal{J}_T, \tag{22b}$$

$$\mathbf{p}_i = \begin{bmatrix} \gamma_i & z_i & d_i & p_i^s \end{bmatrix}^T, \quad \forall i \in \mathcal{J}_T, \tag{22c}$$

where V_i is the volume at node i; p_i is the pressure at node i; H_i is the hydraulic head at node i; h_i is the liquid level at node i; γ_i is the specific weight at node i; z_i is the elevation at node i; d_i is the demand at node i; and p_i^s is the surface pressure at the surface of node i. For discharge nodes $\mathcal{J}_D$, we have:

$$\mathbf{z}_i = \begin{bmatrix} H_i & d_i^o \end{bmatrix}^T, \quad \forall i \in \mathcal{J}_D, \tag{23a}$$

$$\mathbf{u}_i = \begin{bmatrix} d_i \end{bmatrix}^T, \quad \forall i \in \mathcal{J}_D, \tag{23b}$$

$$\mathbf{w}_i = \begin{bmatrix} c_i \end{bmatrix}^T, \quad \forall i \in \mathcal{J}_D, \tag{23c}$$

$$\mathbf{p}_i = \begin{bmatrix} \gamma_i & z_i & p_i \end{bmatrix}^T, \quad \forall i \in \mathcal{J}_D, \tag{23d}$$

where d_i^o is the oil demand at node i, and c_i is the concentration of dispersed oil at node i. As for well nodes $\mathcal{J}_W$,

$$\mathbf{z}_i = \begin{bmatrix} p_i & H_i & d_i \end{bmatrix}^T, \quad \forall i \in \mathcal{J}_W, \tag{24a}$$

$$\mathbf{p}_i = \begin{bmatrix} \gamma_i & z_i & p_i^r & J_i \end{bmatrix}^T, \quad \forall i \in \mathcal{J}_W, \tag{24b}$$

where p_i^r is the reservoir pressure at node i; J_i is the injectivity index at node i. For an individual arc $l \in \mathcal{L}$, we define its vectors as follows. For discharging lines $\mathcal{L}_D$,

$$\mathbf{z}_i = \begin{bmatrix} H_l^L & q_l \end{bmatrix}^T, \quad \forall l \in \mathcal{L}_D, \tag{25a}$$

where H_l^L is the headloss at arc l; and q_l is the volumetric flow rate at arc l. Lastly, for pumping facilities $\mathcal{L}_P$,

$$\mathbf{z}_l = \begin{bmatrix} H_l^L & W_l \end{bmatrix}^T, \quad \forall l \in \mathcal{L}_P, \tag{26a}$$

$$\mathbf{u}_l = \begin{bmatrix} q_l \end{bmatrix}^T, \quad \forall l \in \mathcal{L}_P, \tag{26b}$$

$$\mathbf{p}_l = \begin{bmatrix} \gamma_l \end{bmatrix}^T, \quad \forall l \in \mathcal{L}_P, \tag{26c}$$

and W_l is the hydraulic power demand at arc l. We use the convention that removal of PW from node i is represented by a positive value for demand (*i.e.* $d_i \geq 0$), while a negative value would mean addition of PW (*i.e.* $d_i \leq 0$). The same logic is applied for loss of hydraulic head. Loss of hydraulic head at arc l is shown as a positive value (*i.e.* $H_l^L \geq 0$), while gain of hydraulic head is negative (*i.e.* $H_l^L \leq 0$).

Table 3
Elements present in each nodal-arc set.

Sets	Elements
$\mathcal{J}_T$	{1}
$\mathcal{J}_D$	{2}
$\mathcal{J}_W$	{3,4}
$\mathcal{L}_D$	{(1,2)}
$\mathcal{L}_P$	{(1,3), (1,4)}

6.2. Model and optimization

The PWRI facility considered in this work can be seen in Fig. 2. In it, one can see that PW coming from upstream enters the degasser, which is the last separation equipment. From there, PW can be discharged towards the ocean by flowing through the discharging lines. In addition, it is also possible to re-inject PW at well 1 and 2. To do so, PW needs to go through the pumping facility. Another element shown in the image is the oil in water sensor, which is located downstream of the degasser as specified by regulations. The aforementioned facility is based on a real system currently in operation at the NCS.

This system is described as a graph network $\mathcal{G} = (\mathcal{J}, \mathcal{L})$, containing 4 nodes and 3 arcs. It was considered that node 1 is a tank; node 2 is a discharge; and node 3 and 4 are wells. Moreover, we define arc (1,2) as a discharging line, and arcs (1,3) and (1,4) as pumping facilities. These definitions can be found in Table 3, where the elements of the facility are described in terms of nodes and arcs.

We are mainly interested in investigating the inclusion of FWMC to an EMPC framework. Therefore, the following simplifications have been considered in the formulation of this system model:

1. PW is considered an incompressible liquid. Moreover, oil content in PW density is neglected, implying that γ is constant.
2. Energy balance is replaced by mechanical energy balance as it is assumed that PW does not suffer change of phases, there is no chemical reaction, and change in temperature is negligible.
3. The hydraulic head H_i is formed by pressure head, elevation head, and kinetic head. The kinetic head term is neglected as it is relatively smaller than the other terms.
4. Inflow performance relationship (IPR) correlates the volumetric flowrate of PW re-injection with pressure in the near-wellbore area of a well. We assume a linear function for the IPR as it is observed in practice an almost-linear relationship for single-phase fluids (Jansen, 2017).
5. Each pumping system has one fixed-speed pump, one variable-speed pump and one throttling valve in series. The operational point of the pumping system is given by the intersection between both pumping and system curve (Gülich, 2014). We assume that the pumping system is not constraining the network operation. Thus, we disregard imposing restrictions from its operational envelope, and assume that it is possible to obtain the desired head during operation.

It is desired to operate the PWRI facility with minimal energy consumption. For that, we select an objective function based on the sum of the hydraulic power required by each pumping facility,

$$\Phi = \int \sum_{(i,j) \in \mathcal{L}_P} W_{(i,j)} \, dt \tag{27}$$

where Φ is the objective function to be minimized, with hydraulic power given by:

$$W_l = -\gamma_l H_l^L q_l, \quad \forall l \in \mathcal{L}_P. \tag{28}$$

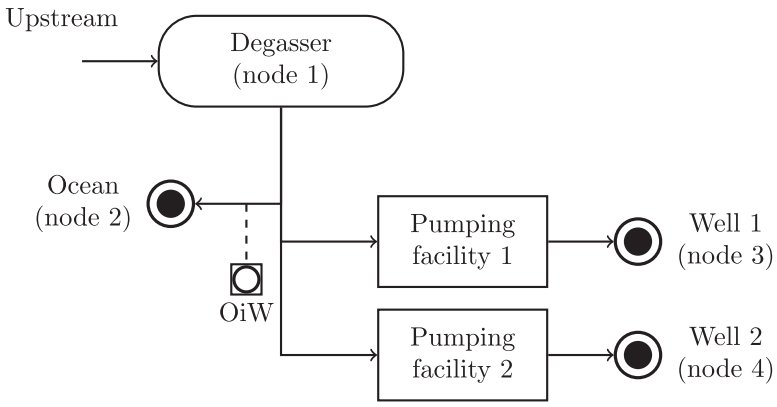

Fig. 2. Produced water re-injection system (PWRI).

Monitoring is performed through means of FWMC. This indicator is traditionally used to estimate the discharged oil concentration from a PWRI facility during a particular time-interval. In the NCS, regulators enforce a calendar-month evaluation of the FWMC, which is represented as follows,

$$\tilde{c}_i(t_m, t_{m+1}) = \frac{\int_{t_m}^{t_{m+1}} c_i(t) d_i(t)\ dt}{\int_{t_m}^{t_{m+1}} d_i(t)\ dt} \leq \tilde{c}_i^{ub}, \quad \forall i \in J_D \tag{29}$$

where $\tilde{c}_i(t_m, t_{m+1})$ is the fixed-time FWMC of dispersed oil in PW discharged at node i. Conservation of mass must be ensured at each node $\mathcal{J}$ of the PW distribution network. While a tank has the capability of storing PW, the same cannot be said about the other nodes. Therefore, their mass balances are given as,

$$\dot{V}_i = \sum_{i \neq jj \in \mathcal{J}} \left(q_{(j,i)} - q_{(i,j)}\right) - d_i, \quad \forall i \in \mathcal{J}_T \tag{30a}$$

$$0 = \sum_{i \neq jj \in \mathcal{J}} \left(q_{(j,i)} - q_{(i,j)}\right) - d_i, \quad \forall i \in \mathcal{J} \setminus \mathcal{J}_T \tag{30b}$$

The mechanical energy balance for the PWRI facility is fulfilled by applying the following relation at each arc $\mathcal{L}$,

$$H_i - H_j = H^L_{(i,j)}, \quad \forall (i,j) \in L, \tag{31}$$

where Eq. (31) states that arcs $\mathcal{L}$ are responsible for adding or removing energy from the PW. To use Eq. (31), it is necessary to define the hydraulic head or piezometric head H_i. The hydraulic head H_i represents the mechanical energy per unit weight of PW at node i. For tanks $\mathcal{J}_T$ and other nodes $\mathcal{J} \setminus \mathcal{J}_T$, the hydraulic head H_i can be obtained by using the relations below,

$$H_i = \frac{p_i^s}{\gamma_i} + (z_i + h_i - z_o), \quad \forall i \in \mathcal{J}_T, \tag{32}$$

$$H_i = \frac{p_i}{\gamma_i} + (z_i - z_o), \quad \forall i \in \mathcal{J} \setminus \mathcal{J}_T, \tag{33}$$

where z_o is a reference elevation, which we assume to be given by the lowest elevation node $i \in \mathcal{J}$. We stress that hydraulic head H_i is calculated differently in Eqs. (32) and (33) as changes in the PW content of tank nodes $\mathcal{J}_T$ occur. As one may notice, equation (30a) is in terms of volume, while Eq. (30b) is in terms of level. The conversion between volume and level of liquid at a tank node $\mathcal{J}_T$ can be done with the following equation,

$$V_i = f_i(h_i), \quad \forall i \in \mathcal{J}_T \tag{34}$$

where f_i is the conversion map of liquid into volume at tank i. IPR is commonly used to represent the relation between re-injected volumetric flowrate and the pressure in the near-wellbore area of a well (Jansen, 2017). It can be obtained experimentally by operators through injectivity tests, which are performed individually at each re-injection well. Thus, for well nodes $\mathcal{J}_W$ we use the following expression,

$$p_i = p_i^r + \frac{d_i}{J_i}, \quad \forall i \in \mathcal{J}_W \tag{35}$$

where p_i^r is the reservoir pressure; and J_i is the injectivity index.

Table 4
Parameters for the nodes used in the case study.

Variable	Unit	Bound	Node			
			1	2	3	4
d	m^3/s	upper	-	inf	0.1389	0.255
		value	−0.305	-	-	-
		lower	-	0	0.0833	0.159
H	m	upper	inf	inf	inf	inf
		value	-	-	-	-
		lower	0	0	0	0
p	kPa	upper	inf	-	inf	inf
		value	-	101.3	-	-
		lower	0	-	0	0
p^s	kPa	upper	-	-	-	-
		value	103.3	-	-	-
		lower	-	-	-	-
V	m^3	upper	52.60	-	-	-
		value	-	-	-	-
		lower	39.09	-	-	-
h	%	upper	50	-	-	-
		value	-	-	-	-
		lower	40	-	-	-
$z - z_0$	m	upper	-	-	-	-
		value	323.25	310.193	40.2	0
		lower	-	-	-	-

7. Case study

In this paper, we study the problem of produced water management optimization in an oil and gas produced water re-injection network. We want to demonstrate the benefits of using the FWMC-EMPC as a tool to manage the monthly oil content discharged to the ocean. The PWRI facility considered in this case study has been described in the previous section. Its configuration is shown in Fig. 2, and Table 3. The objective is to minimize (27). The system behavior is described by the set of variables (21) and Eqs. (28)–(35). The parameters used in this simulation as well as the bounds of the decision variables are shown in Tables 4 and 5. The demand at each well is bounded due to requirements introduced by reservoir engineers. Furthermore, all nodes must have a hydraulic head greater than zero. This is doable for two reasons: first, we are using absolute pressure instead of barometric pressure; and second, the lowest elevation is chosen for reference.

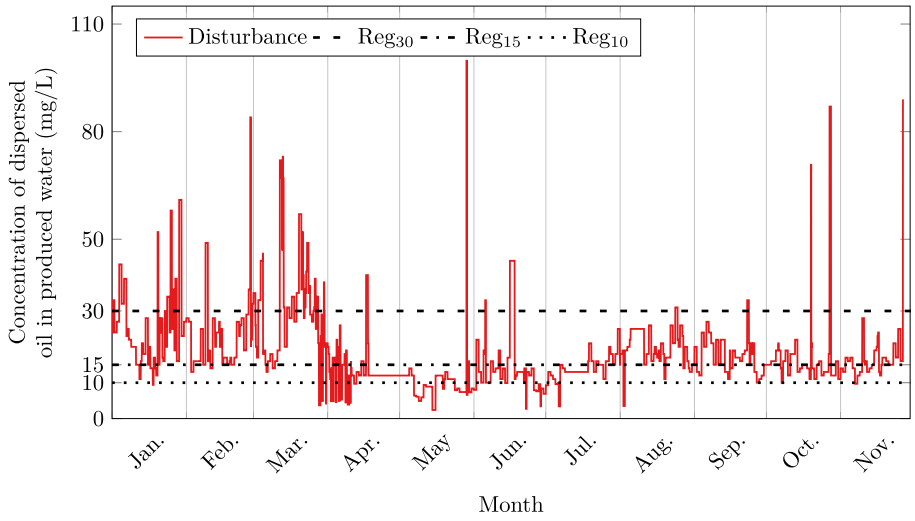

Fig. 3. Disturbance profile of the concentration of dispersed oil in produced water (PW). The disturbance is shown in red line. The 30 mg/L regulation is shown as a dashed black line. The 15 mg/L regulation is shown as a dash-dotted black line. The 10 mg/L regulation is shown as a dotted black line. (For interpretation of the references to colour in this figure legend, the reader is referred to the web version of this article.)

Table 5
Parameters for the arcs during this case study.

Variable	Unit	Bound	Arc		
			(1,2)	(1,3)	(1,4)
H^L	m	upper	inf	0	0
		value	-	-	-
		lower	0	-inf	-inf
q	m^3/s	upper	inf	inf	inf
		value	-	-	-
		lower	0	0	0
W	W	upper	0	inf	inf
		value	-	-	-
		lower	-inf	0	0

Disturbances on the dispersed oil in PW are considered to affect the process at the beginning of each day. Its profile is shown in Fig. 3, where for reference we trace the limits for the monthly FWMC according to three regulations: 30 mg/L; 15 mg/L and 10 mg/L. During this time period, it is possible to see that the treatment facility delivers a wide range of different concentrations of dispersed oil in PW. These concentrations range from values below 10 mg/L to values above 30 mg/L. It is evident that the chosen regulation and the delivered concentration of dispersed oil should have major influence over decisions taken by an optimal control strategy. We formulate three case studies, where it is desired to operate with the monthly FWMC of dispersed oil in discharged PW below a particular threshold. These limits were selected based on the current regulation and on possible future regulations (Steinar et al., 2016). This translates into case studies with the following monthly regulations: 30 mg/L (reg_{30}), 15 mg/L (reg_{15}), and 10 mg/L (reg_{10}).

To benchmark the performance of the FWMC-EMPC controller (eFWMC), we consider three other controllers. These controllers are referred to as: greedy EMPC (gEMPC); soft-constrained FWMC-EMPC (sFWMC); and conservative EMPC (cEMPC). The gEMPC controller sets a lower limit, or floor, to the energy consumption as it was designed to present an ideal consumption of energy. To achieve that, the gEMPC controller ignores any constraint associated with the environmental regulation. We refer to this optimal controller as OCP_G, which is constructed with Eqs. (9a)–(9f). The cEMPC controller was designed to guarantee that criterion (i) of Theorem 1 always hold without predictions for the expanding-time FWMC. In the cEMPC controller, a simple logic checks if $c(t) \in \tilde{\mathbb{C}}$. If this is true, OCP_G is solved. Otherwise, OCP_R is the one being solved. The sFWMC controller was developed partially based on the eFWMC controller. For instance the sFWMC controller solves only the OCP_S and does not use Algorithm 1. Therefore, it is a direct competitor to the eFWMC controller. We compare the economic and environmental performance of the closed-loop system under each controller for the three aforementioned case studies. The performance is given by the metrics: total pumping energy, total PW discharged, total oil discharged, and violation of regulation in months. We state that any viable control strategy should lead to zero violations of regulation, and should lead to a total pumping energy that stays between the gEMPC and the cEMPC controllers. To solve the OCP associated with each strategy, direct transcription is performed, generating a nonlinear program (NLP). For that, we use direct collocation with a third order Radau scheme. The NLP problems are developed in *CasADi* v.3.5.1 (Andersson et al., 2019) using *Python* 3.7.1 and solved with *IPOPT* (Wchter and Biegler, 2006) version 3.12.3 with mumps linear solver on a 2.2Ghz workstation with 16GB memory. In the simulations, the plant system is integrated by using the *IDAS* integrator (Hindmarsh et al., 2005). The total time of simulation (t_{sim}) is 330 days. In addition, for all the strategies, a 24 h prediction time and 1 h time-step are considered. Moreover, process information is gathered hourly through measurements. We assume that all states and disturbances are measured, that there is no plant-model mismatch and that there is an ideal basic controller.

8. Results and discussion

8.1. Economic and environmental performance

The economic and environmental performance of the closed-loop associated with strategies gEMPC, sFWMC, eFWMC and cEMPC are shown in Table 6.

When considering all the simulated case-studies, one can see that the gEMPC strategy uses the lowest amount of pumping energy, and discharges the highest quantity of PW and oil towards the ocean. This was expected as the gEMPC strategy was formulated without any concern regarding the PW environmental regulation. The cEMPC strategy, different from the gEMPC strategy, requires the highest amount of pumping energy, and discharges

Table 6
Comparison between the different case-studies considered in this work. We have total pumping energy, total produced water (PW) discharged to the ocean, total oil discharged to the ocean, and number of months when violation of the regulation has occurred. The time of simulation is 330 days.

Case study	Total pumping energy ($\times 10^3$ GJ)	Total PW discharged ($\times 10^3$ m^3)	Total oil discharged ($\times 10^3$ kg)	Violation of regulation (months)
gEMPC	60.41	1790.15	32.55	(many)
$sFWMC_{30}$	60.80	1766.95	31.59	0
$eFWMC_{30}$	60.85	1763.82	31.49	0
$cEMPC_{30}$	63.07	1630.36	25.71	0
$sFWMC_{15}$	69.98	1212.00	16.66	3
$eFWMC_{15}$	71.46	1121.37	14.94	0
$cEMPC_{15}$	75.39	887.95	10.46	0
$sFWMC_{10}$	80.14	600.30	7.35	7
$eFWMC_{10}$	85.23	292.51	2.70	0
$cEMPC_{10}$	86.65	209.05	1.58	0

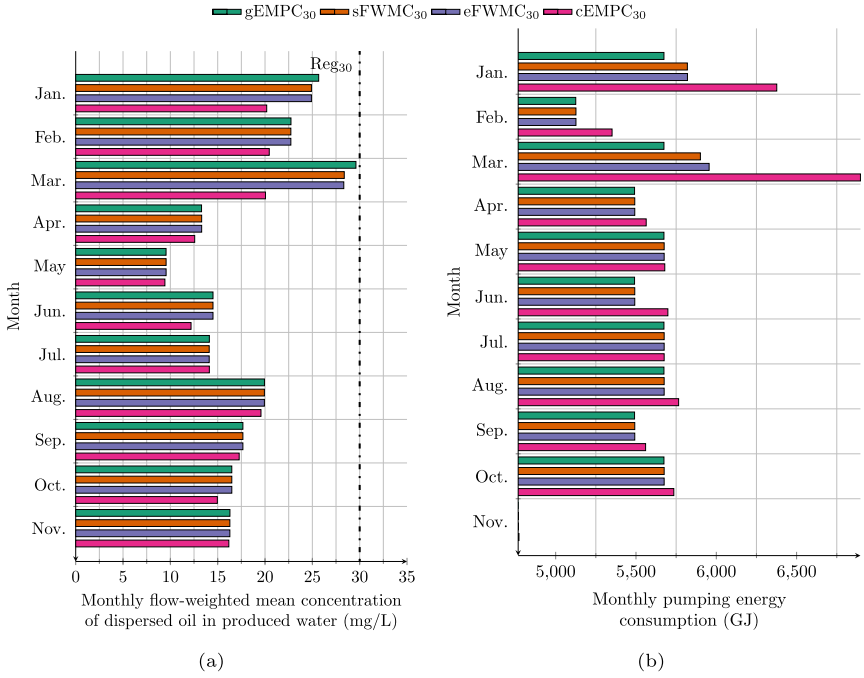

Fig. 4. Monthly comparison of the FWMC of dispersed oil in PW and the pumping energy consumption considering a 30 mg/L regulation. $gEMPC_{30}$ strategy is shown as green bars. $sFWMC_{30}$ strategy is shown as orange bars. $eFWMC_{30}$ strategy is shown as purple bars. $cEMPC_{30}$ is shown as magenta bars. (For interpretation of the references to colour in this figure legend, the reader is referred to the web version of this article.)

the least quantity of PW and oil towards the ocean. The performance of the remaining strategies can be placed within the performance of the gEMPC and cEMPC strategies. We stress that while the sFWMC strategy shows a slightly better economic performance than the eFWMC strategy, the first also presents a worse environmental performance than the second. Moreover, the sFWMC strategy was unable to deal with the imposed environmental regulations for stricter cases. Simulation shows that a decrease in PW discharges can only be achieved by re-injecting more PW in the re-injection wells. As expected, there is a trade-off between energy consumption, and discharge of PW and oil. This trade-off seems to follow a certain proportionality when it is related to the PW discharge. Nevertheless, the same is not observed for the oil discharges as the dispersed oil concentration have an important role on quantifying the total oil discharge. We continue our investigation into the different strategies by considering the monthly FWMC of dispersed oil in discharged PW, and the monthly pumping energy consumption for the 30 mg/L and the 10 mg/L case-studies. These case-studies summarize well the different aspects of the considered strategies. We start by analyzing the 30 mg/L case-study. Then, continue with the 10 mg/L case-study. Fig. 4 displays both the monthly FWMC of dispersed oil in discharged PW (a), and the monthly pumping energy consumption (b) for the 30 mg/L case-study. Fig. 4a shows that the minimum performance standard of 30 mg/L was successfully achieved for all strategies. It is possible to see the impact of each strategy over the monthly FWMC of dispersed oil in PW. In general, we observe that the $gEMPC_{30}$ strategy had the same performance as strategies $sFWMC_{30}$ and $eFWMC_{30}$ for several months. On the other hand, $cEMPC_{30}$ is the strategy with the lowest values for the monthly FWMC of dispersed oil in PW. Regarding monthly pumping energy consumption, Fig. 4b shows that the $sFWMC_{30}$ and $eFWMC_{30}$ strategies consume more energy than the $gEMPC_{30}$ strategy in January and March. For all the other months of the simulation, the $sFWMC_{30}$ and $eFWMC_{30}$ strategies consume the same amount of energy as the $gEMPC_{30}$ strategy. In addition, we highlight that the $cEMPC_{30}$ consumes more energy than the other strategies for most months.

In Fig. 5, the results for the monthly FWMC of dispersed oil in PW (a), and the monthly pumping energy consumption (b) for the 10 mg/L case-study are showed. It is observed in Fig. 5a that the gEMPC10 strategy achieves the minimum performance requirement only once in eleven months. The sFWMC10 strategy fails to achieve the minimum standard performance in seven of the eleven simulated months. The remaining strategies have succeeded in sat-

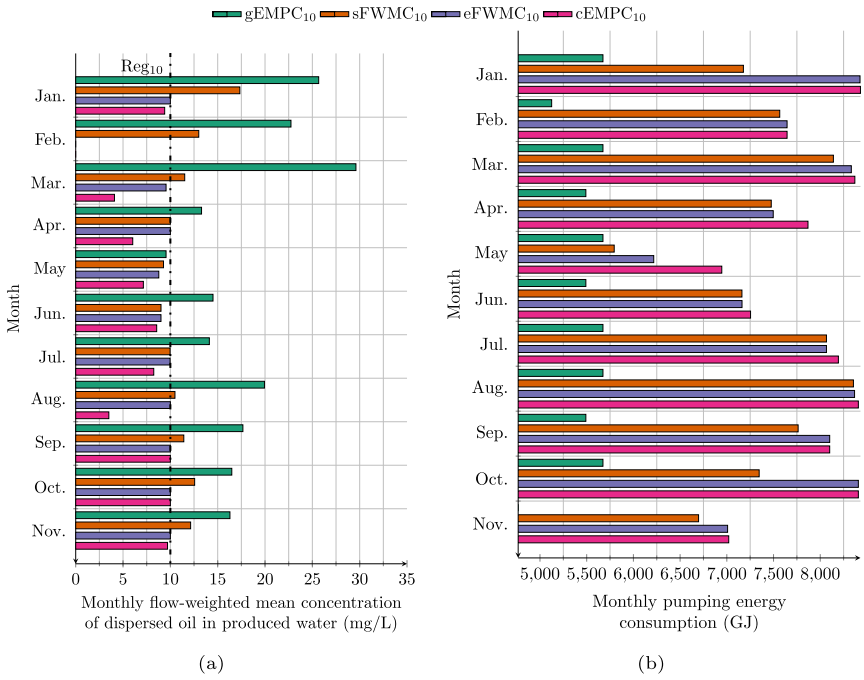

Fig. 5. Monthly comparison of the FWMC of dispersed oil in PW and the pumping energy consumption considering a 10 mg/L regulation. $gEMPC_{10}$ strategy is shown as green bars. $sFWMC_{10}$ strategy is shown as orange bars. $eFWMC_{10}$ strategy is shown as purple bars. $cEMPC_{10}$ is shown as magenta bars. (For interpretation of the references to colour in this figure legend, the reader is referred to the web version of this article.)

isfying the environmental regulation. As no discharge has occurred in February for both the eFWMC10 and cEMPC10 strategies, we chose to set their values at 0 mg/L. Fig. 5b shows the results regarding the monthly pumping energy consumption and, differently from the 30 mg/L case-study, no similarity in performance is observed for the $gEMPC_{10}$, $sFWMC_{10}$ and $eFWMC_{10}$ strategies. In fact, the energy requirement of the $eFWMC_{10}$ and $cEMPC_{10}$ strategies are similar regarding pumping energy consumption. When comparing the $sFWMC_{10}$ and the $eFWMC_{10}$ strategy, the energy consumption of the former was either equal or lower than the latter. Admittedly, for May, the $sFWMC_{10}$ strategy was able to respect the environmental regulation, while reducing energy consumption considerably.

The results from May shown in Fig. 5 are a clear example that enforcing criterion (i) of Theorem 1 in the closed-loop system through the eFWMC strategy might provoke a negative impact in the closed-loop energy consumption due to conservatism of criterion (i). Despite that, strategy eFWMC is considered a viable strategy as no regulation was infringed, and its economic performance is within the performance of the gEMPC and cEMPC strategies.

8.2. On the piecewise expanding-time FWMC trajectory

The PWRI facility manages where the treated PW should be disposed, but it has by no means any capability of reducing the concentration of dispersed oil in PW. Nevertheless, we have shown in the previous section that, depending on how the re-injection facility is operated, it is capable of reducing the monthly FWMC of dispersed oil in discharged PW. In this section, we want to elucidate the behavior of the closed-loop piecewise expanding-time FWMC (11e), which is shown in Fig. 6. The beginning of a month (t_m) is represented by hollow circles, while the end (t_{m+1}) is shown as filled circles. Moreover, we have assigned the value 0 mg/L at times in which the piecewise expanding-time FWMC is indeterminate.

For the gEMPC strategy, the trajectory of $\tilde{c}(t)$ remained the same for each case study. This was expected as the gEMPC strategy is insensitive to changes in both the FWMC regulation and in the concentration of dispersed oil in PW. Therefore, the violation of the regulation depends exclusively on the performance of the PW separation facility. In the sFWMC strategy, the OCP_S is always being solved. In the beginning of a month, we have that $\mathbf{V}(t_m, t) = 0$. As discussed earlier, this condition may lead NLP_S to lose its LICQ. One can observe that in the beginning of a month, the sFWMC strategy starts either at the same point as the gEMPC strategy or at 0 mg/L. For the latter, a spike towards the gEMPC trajectory was soon observed, which is an indicative that the sFWMC strategy is sensitive at the beginning of a month. As seen in Fig. 6b and c, these sudden spikes have caused $\tilde{c}(t)$ to leave the feasible region $\tilde{\mathbb{C}}$. Due to the presence of soft-constraints in NLP_S, strategy sFWMC tries to steer $\tilde{c}(t)$ back to the feasible region $\tilde{\mathbb{C}}$. Although the sFWMC strategy succeeded for some months, this success depends on future realizations of the oil concentration in dispersed oil delivered by the PW separation facility. For all case-studies, the eFWMC strategy has led $\tilde{c}(t)$ to stay always within the feasible region $\tilde{\mathbb{C}}$. Algorithm 1 prioritizes solving OCP_R while criterion (i) is not being satisfied in the closed-loop system. An indicative that OCP_R is being solved is the overlap between the eFWMC and cEMPC strategy at 0 mg/L, as observed in Fig. 6. Once criterion (i) has been met for the first time, Algorithm 1 started solving OCP_F until a new month begin. Overall, the results presented above show the importance of Algorithm 1 for the success of strategy eFWMC.

8.3. On states and control inputs trajectory

We show the closed-loop behavior of the ocean discharge, re-injection at well 1 and re-injection at well 2 on Fig. 7 for the 15 mg/L case-study. We only focus on this case-study as it captures well the behavior seen for other case-studies.

For the gEMPC strategy, all the control actions are kept constant for the whole simulation period. Moreover, PW re-injection flowrates are kept always at their respective lower bounds. When considering the cEMPC strategy, one may notice that it operates

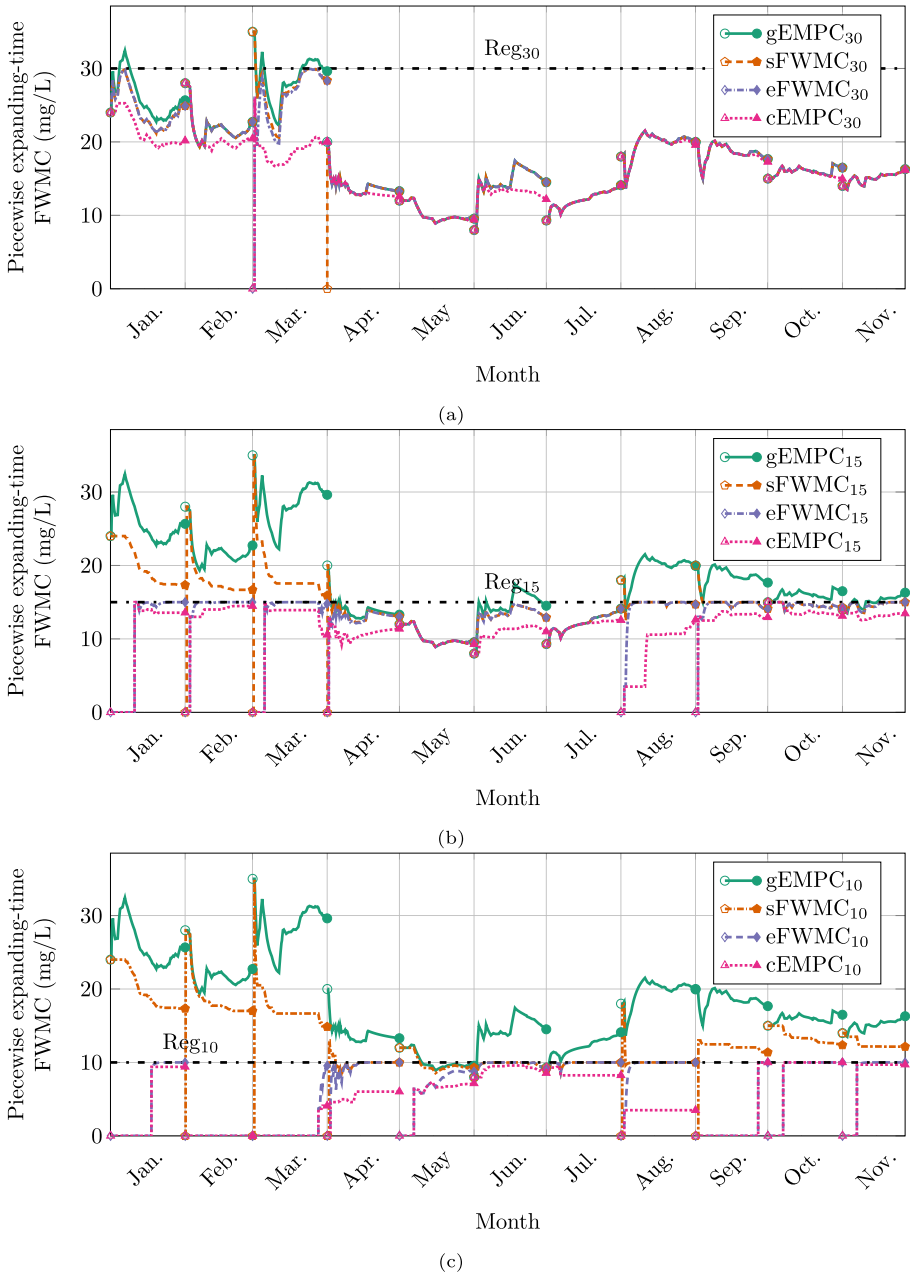

Fig. 6. Closed-loop trajectory of the piecewise expanding-time FWMC of dispersed oil in produced water. The beginning and the end of each month is represented respectively with a hollow symbol and filled symbol. Strategy gEMPC is shown as a green solid line with circles; strategy sFWMC is shown as an orange dashed line with pentagons; strategy eFWMC is shown as a purple dash-dotted line with diamonds; and strategy cEMPC is shown as a magenta dotted line with triangles. All regulations are shown as a dash-dotted black line. (For interpretation of the references to colour in this figure legend, the reader is referred to the web version of this article.)

at extremes, with a bang-bang behavior. This occurs as there are frequent changes between OCP_G and OCP_R for the cEMPC strategy due to the logic switch. In addition, for both strategies, the tank volume was kept at its maximum.

From the sFWMC strategy, one can clearly see that some spikes in ocean discharge occurred at certain months. As seen in the last subsection, $\tilde{c}(t)$ leaves the feasible region $\tilde{\mathbb{C}}$ in the beginning of those months. Once it becomes possible for $\tilde{c}(t)$ to approach the feasible region $\tilde{\mathbb{C}}$, strategy sFWMC increases ocean discharge drastically, causing the spikes observed in Fig. 7a. As no addition PW is entering the facility, the sFWMC strategy uses the PW stored in the tank to lead $\tilde{c}(t)$ towards $\tilde{\mathbb{C}}$ faster. Nevertheless, this can only be done for a short time as the tank volume transits from its maximum volume to its minimum volume.

Generally, the eFWMC strategy has showed trajectories where the transition between maximum and minimum flowrates are smoother than the cEMPC and sFWMC strategies. However, sharp increases in ocean discharge were observed for the eFWMC strategy whenever Algorithm 1 changed from OCP_R to OCP_F. Once NLP_F was selected, flowrate trajectories became smoother as allowed discharge is calculated implicitly due to the presence of the FWMC constraints.

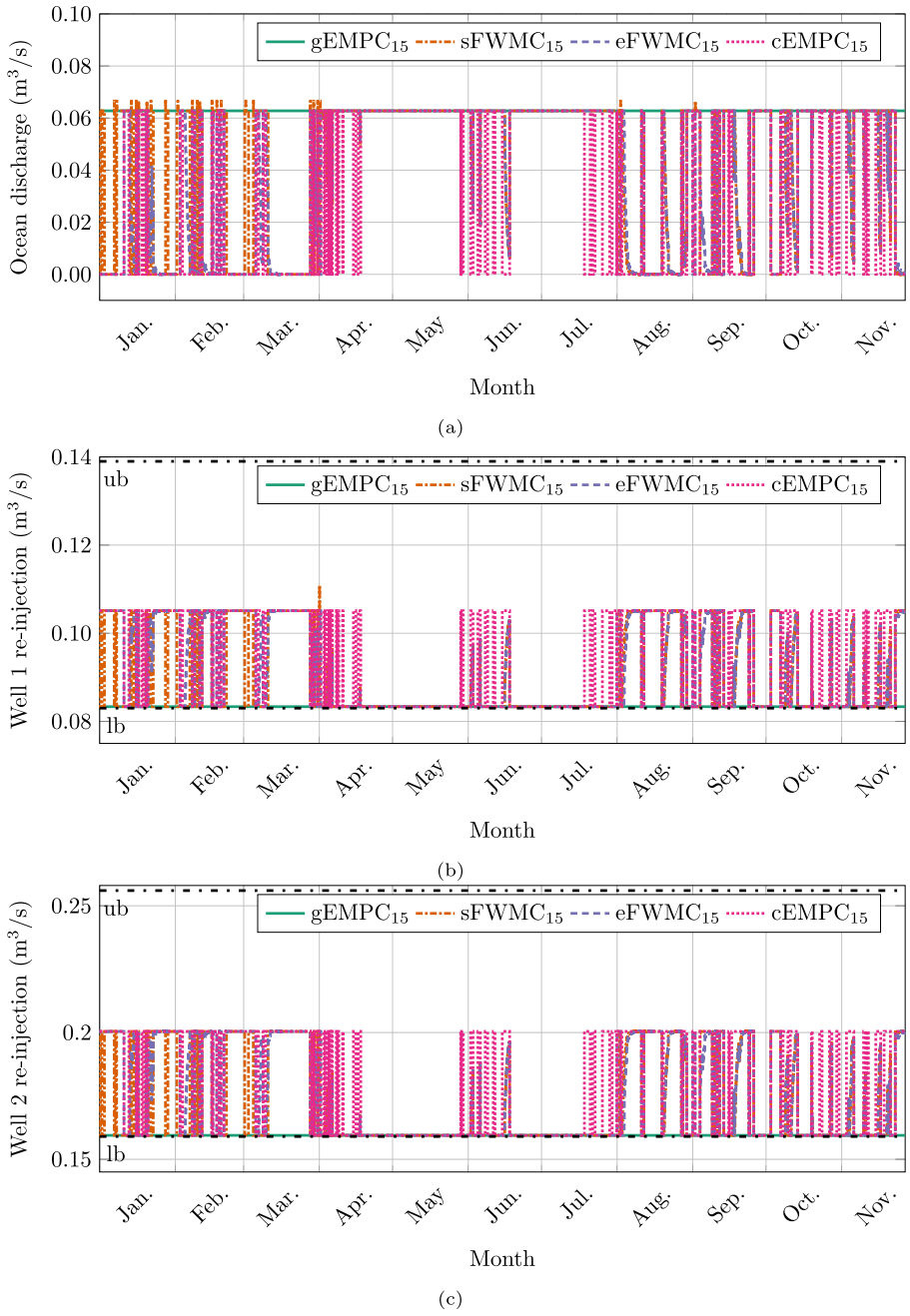

Fig. 7. Closed-loop trajectory of the ocean discharge, well 1 re-injection, and well 2 re-injection flowrates. Strategy gEMPC is a green solid line. Strategy sFWMC is shown as an orange dash-dotted line. Strategy eFWMC is a purple dashed line. Strategy cEMPC is a magenta dotted line. All re-injection bounds are shown as a dash-dotted black line. (For interpretation of the references to colour in this figure legend, the reader is referred to the web version of this article.)

9. Conclusion

In this work we developed a FWMC-EMPC framework to perform PW management at an offshore PWRI facility. The aim was to cope with environmental regulation while minimizing pumping energy consumption, even when disturbances affect the concentration of dispersed oil in PW. The FWMC-EMPC strategy was benchmarked against three other control strategies; their closed-loop economic and environmental performance was obtained by simulating several case-studies with distinct environmental regulations. Overall, the FWMC-EMPC strategy shows several advantages in comparison to the other strategies. First, it is robust as violation of environmental regulation does not occur. Second, it presents adaptability as the control policy is adapted by using historical data information and new concentration measurements. Third, it is flexible since its economic and environmental performance behave similarly to other strategies when circumstances dictate, such as the treatment facility performance and the considered regulation. In conclusion, the FWMC-EMPC framework has shown to be a relevant contribution to the oil and gas industry. Nevertheless, we stress that this framework can be particularly interesting for researchers dealing with effluent disposal in other industries.

Declaration of Competing Interest

The authors declare that they have no known competing financial interests or personal relationships that could have appeared to influence the work reported in this paper.

Acknowledgement

This research is a part of BRU21 NTNU Research and Innovation Program on Digital and Automation Solutions for the Oil and Gas Industry (www.ntnu.edu/bru21) and supported by OKEA ASA. In addition, we would like to acknowledge license partners Neptune Energy Norge AS, and Petoro AS for allowing the usage of field data. The authors would like to thank employees at OKEA Per Magne Bjellvg, Alf Sebastian Lackner, Even Moen Kirkholt, Raymond Hellerud and Katrine Torvik for their valuable input.

References

Andersson, J.A.E., Gillis, J., Horn, G., Rawlings, J.B., Diehl, M., 2019. CasADi : a software framework for nonlinear optimization and optimal control. Math. Program. Comput. 11, 1–36. doi:10.1007/s12532-018-0139-4.

Arai, Y., Koizumi, A., Inakazu, T., Masuko, A., Tamura, S., 2013. Optimized operation of water distribution system using multipurpose fuzzy LP model. Water Sci. Technol. Water Supply 13, 66–73. doi:10.2166/ws.2012.080.

Betts, J.T., 1998. Survey of numerical methods for trajectory optimization. J. Guid. Control Dyn. 21, 193–207. doi:10.2514/2.4231.

Beyer, J., Bakke, T., Lichtenthaler, R., Klungsøy, J., 2019. Environmental Effects of Offshore Produced Water Discharges Evaluated for the Barents Sea. Technical Report. www.niva.no

Beyer, J., Goksøyr, A., Øystein Hjermann, D., Klungsøyr, J., 2020. Environmental effects of offshore produced water discharges: a review focused on the norwegian continental shelf. Mar. Environ. Res. 162. doi:10.1016/j.marenvres.2020.105155.

Biegler, L.T., 2010. Nonlinear Programming, Vol. 22. Society for Industrial and Applied Mathematics doi:10.1137/1.9780898719383.

Commision, O., 2001. Recommendation 2001/1 for the Management of Produced Water from Offshore Installations. Technical Report. OSPAR Comission. http://rod.eionet.europa.eu/obligations/488/legislation

Das, T., Jäschke, J., 2018. Modeling and control of an inline deoiling hydrocyclone. IFAC-PapersOnLine 51, 138–143. doi:10.1016/j.ifacol.2018.06.368.

Das, T., Jäschke, J., 2019. Simplified first-principles model of a compact flotation unit for use in optimization and control. Ind. Eng. Chem. Res. 58, 1273–1285. doi:10.1021/acs.iecr.8b04018.

Ellis, M., Durand, H., Christofides, P.D., 2014. A tutorial review of economic model predictive control methods. J. Process Control 24, 1156–1178. doi:10.1016/j.jprocont.2014.03.010.

Farajzadeh, R., Kahrobaei, S.S., Zwart, A.H.D., Boersma, D.M., 2019. Life-cycle production optimization of hydrocarbon fields: thermoeconomics perspective. Sustain. Energy Fuels 3, 3050–3060. doi:10.1039/c9se00085b.

Faulwasser, T., Grüne, L., Müller, M.A., 2018. Economic nonlinear model predictive control. Foundations Trends Syst. Control 5, 1–98. doi:10.1561/2600000014.

Ferreau, H.J., Almer, S., Peyrl, H., Jerez, J.L., Domahidi, A., 2016. Survey of industrial applications of embedded model predictive control. IEEE, p. 601. doi:10.1109/ECC.2016.7810351.

Foss, B., Knudsen, B.R., Grimstad, B., 2018. Petroleum production optimization a static or dynamic problem? Comput. Chem. Eng. 114, 245–253. doi:10.1016/j.compchemeng.2017.10.009.

Grema, A.S., Cao, Y., 2013. Optimization of petroleum reservoir waterflooding using receding horizon approach. In: Proceedings of the 2013 IEEE 8th Conference on Industrial Electronics and Applications, ICIEA 2013, pp. 397–402. doi:10.1109/ICIEA.2013.6566402.

Grema, A.S., Cao, Y., 2016. Optimal feedback control of oil reservoir waterflooding processes. Int. J. Autom. Comput. 13, 73–80. doi:10.1007/s11633-015-0909-7.

Gülich, J.F., 2014. Centrifugal Pumps, Vol. 9783642401. Springer-Verlag Berlin Heidelberg.

Hindmarsh, A.C., Brown, P.N., Grant, K.E., Lee, S.L., Serban, R., Shumaker, D.E., Woodward, C.S., 2005. Sundials: suite of nonlinear and differential/algebraic equation solvers. ACM Trans. Math. Softw. 31, 363–396. doi:10.1145/1089014.1089020.

Hourfar, F., Moshiri, B., Salahshoor, K., Elkamel, A., 2017. Real-time management of the waterflooding process using proxy reservoir modeling and data fusion theory. Comput. Chem. Eng. 106, 339–354. doi:10.1016/j.compchemeng.2017.06.018.

Hrovat, D., Cairano, S.D., Tseng, H.E., Kolmanovsky, I.V., 2012. The development of model predictive control in automotive industry: a survey. In: Proceedings of the IEEE International Conference on Control Applications, pp. 295–302. doi:10.1109/CCA.2012.6402735.

Jansen, J.-D., 2017. Nodal analysis of oil and gas production systems.

Judd, S., Qiblawey, H., Al-Marri, M., Clarkin, C., Watson, S., Ahmed, A., Bach, S., 2014. The size and performance of offshore produced water oil-removal technologies for reinjection. Sep. Purif. Technol. 134, 241–246. doi:10.1016/j.seppur.2014.07.037.

Kadam, J.V., Marquardt, W., 2007. Integration of economical optimization and control for intentionally transient process operation. Lect. Notes Control Inf. Sci. 358, 419–434. doi:10.1007/978-3-540-72699-9_34.

Kerrigan, E. C., Maciejowski, J. M., 2000. Soft constraints and exact penalty functions in model predictive control.

Kulovic, N., 2020. Norways ministry of petroleum and energy on thursday launched the countrys 25th licensing round, encompassing 136 blocks in the norwegian sea and the Barents Sea off norway.https://www.offshore-energy.biz/norway-turns-the-spotlight-on-barents-sea-in-25th-licensing-round/.

Kurek, W., Ostfeld, A., 2014. Multiobjective water distribution systems control of pumping cost, water quality, and storage-reliability constraints. J. Water Resour. Plann. Manage. 140, 184–193. doi:10.1061/(asce)wr.1943-5452.0000309.

Mala-Jetmarova, H., Sultanova, N., Savic, D., 2017. Lost in optimisation of water distribution systems? A literature review of system operation. Environ. Modell. Softw. 93, 209–254. doi:10.1016/j.envsoft.2017.02.009.

Mayne, D., Michalska, H., 1988. Receding horizon control of nonlinear systems. IEEE, pp. 464–465. doi:10.1109/CDC.1988.194354.

Miljødirektoratet, 2015. Utredning av beste tilgjengelige teknikker (BAT) for rensing av produsert vann som slippes ut fra petroleumsvirksomheten til havs. Technical Report. Miljdirektoratet. https://www.miljodirektoratet.no/publikasjoner/2015/desember-2105/utredning-av-beste-tilgjengelige-teknikker-for-rensing-av-produsert-vann-som-slippes-ut-fra-petroleumsvirksomheten-til-havs/

Morari, M., Maeder, U., 2012. Nonlinear offset-free model predictive control. Automatica 48, 2059–2067. doi:10.1016/J.AUTOMATICA.2012.06.038.

Müller, M.A., Angeli, D., Allgöwer, F., 2014. Transient average constraints in economic model predictive control. Automatica 50, 2943–2950. doi:10.1016/j.automatica.2014.10.024.

Nasiri, M., Jafari, I., Parniankhoy, B., 2017. Oil and gas produced water management: a review of treatment technologies, challenges, and opportunities. Chem. Eng. Commun. 204, 990–1005. doi:10.1080/00986445.2017.1330747.

Nocedal, J., Wright, S.J., 2006. Numerical Optimization. Springer New York doi:10.1007/978-0-387-40065-5.

NOROG, 2019. Miljørapport 2019: Olje- og gassindustriens miljøarbeid - Fakta og utviklingstrekk. Technical Report. Norsk olje and gass. https://www.norskoljeoggass.no/contentassets/172447a918d14f13aee01614037954b7/norog-miljorapport19-orig.pdf

Pannocchia, G., 2015. Offset-free tracking MPC: a tutorial review and comparison of different formulations. In: 2015 European Control Conference, ECC 2015, pp. 527–532. doi:10.1109/ECC.2015.7330597.

Qin, S.J., Badgwell, T.A., 2003. A survey of industrial model predictive control technology. Control Eng. Pract. 11, 733–764. doi:10.1016/S0967-0661(02)00186-7.

Rawlings, J.B., Amrit, R., 2009. Optimizing process economic performance using model predictive control. Lect. Notes Control Inf. Sci. 384, 119–138. doi:10.1007/978-3-642-01094-1_10.

Rawlings, J.B., Angeli, D., Bates, C.N., 2012. Fundamentals of economic model predictive control. In: Proceedings of the IEEE Conference on Decision and Control, pp. 3851–3861. doi:10.1109/CDC.2012.6425822.

Smit, M., Hayes, S., Pelz, O., Arnold, R., Brown, W., 2020. New produced water risk based approach guidance. In: Society of Petroleum Engineers - SPE International Conference and Exhibition on Health, Safety, Environment, and Sustainability, pp. 1–15. doi:10.2118/199412-ms.

Steinar, N., Eimund, G., Egil, D., 2016. Produced water management under the norwegian zero harmful discharge regime-benefits with the risk based approach. In: Society of Petroleum Engineers - SPE International Conference and Exhibition on Health, Safety, Security, Environment, and Social Responsibility, pp. 1–9. doi:10.2118/179326-ms.

Stentoft, P.A., Vezzaro, L., Mikkelsen, P.S., Grum, M., Munk-Nielsen, T., Tychsen, P., Madsen, H., Halvgaard, R., 2020. Integrated model predictive control of water resource recovery facilities and sewer systems in a smart grid: example of full-scale implementation in Kolding. Water Sci. Technol. 81, 1766–1777. doi:10.2166/wst.2020.266.

Stokes, C.S., Maier, H.R., Simpson, A.R., 2015. Water distribution system pumping operational greenhouse gas emissions minimization by considering time-dependent emissions factors. J. Water Resour. Plann. Manage. 141. doi:10.1061/(ASCE)WR.1943-5452.0000484.

Suwartadi, E., Krogstad, S., Foss, B., 2015. Adjoint-based surrogate optimization of oil reservoir water flooding. Optim. Eng. 16, 441–481. doi:10.1007/s11081-014-9268-4.

Taha, A., Amani, M., 2019. Overview of water shutoff operations in oil and gas wells; chemical and mechanical solutions. ChemEngineering 3, 1–11. doi:10.3390/chemengineering3020051.

Vallabhan, M., Holden, C., Skogestad, S., 2020. A first-principles approach for control-oriented modeling of de-oiling hydrocyclones. Ind. Eng. Chem. Res. 59, 18937–18950. doi:10.1021/acs.iecr.0c02859.

Viholainen, J., Tamminen, J., Ahonen, T., Ahola, J., Vakkilainen, E., Soukka, R., 2013. Energy-efficient control strategy for variable speed-driven parallel pumping systems. Energy Effic. 6, 495–509. doi:10.1007/s12053-012-9188-0.

Wchter, A., Biegler, L.T., 2006. On the implementation of an interior-point filter line-search algorithm for large-scale nonlinear programming. Math. Program. 106, 25–57. doi:10.1007/s10107-004-0559-y.

Zhang, H., Liang, Y., Zhou, X., Yan, X., Qian, C., Liao, Q., 2017. Sensitivity analysis and optimal operation control for large-scale waterflooding pipeline network of oilfield. J. Pet. Sci. Eng. 154, 38–48. doi:10.1016/j.petrol.2017.04.019.

Zheng, J., Chen, B., Thanyamanta, W., Hawboldt, K., Zhang, B., Liu, B., 2016. Offshore produced water management: a review of current practice and challenges in harsh/arctic environments. Mar. Pollut. Bull. 104, 7–19. doi:10.1016/j.marpolbul.2016.01.004.

Zhou, X., Liang, Y., Xin, S., Di, P., Yan, Y., Zhang, H., 2019. A MINLP model for the optimal waterflooding strategy and operation control of surface waterflooding pipeline network considering reservoir characteristics. Comput. Chem. Eng. 129. doi:10.1016/j.compchemeng.2019.106512.